https://doi.org/10.5564/mgs.v29i59.3409

Mongolian Geoscientist

Original Article

Delineating Plio-Pleistocene channels (gas reservoirs) via seismic attributes in Baltim Gas Field, Nile Delta, Egypt

Ali Saeed Ali El-Sayed[1,2]*, Walid Mohamed Mabrouk[1], Ahmed Mohsen Metwally[1]

[1]Geophysics Department, Faculty of Science, Cairo University, Giza, 12613, Egypt
[2]Petrobel Petroleum Company, Cairo, 11823, Egypt
*Corresponding author: ayehia2@petrobel.org, ORCID: 0009-0009-6432-485X

ARTICLE INFO

Article history:

Received: 12 July, 2024
Revised: 04 December, 2024
Accepted: 09 December, 2024

ABSTRACT

The Baltim gas fields in the offshore Nile Delta contain substantial gas condensate accumulations. This study aims to identify Pleistocene (El-Wastani formation) and Pliocene (Kafr El-Sheikh formation) reservoirs. Data from five wells, including gamma-ray, density, neutron, sonic, and resistivity wireline logs, were integrated with seismic data to refine gas horizon interpretation. A synthetic seismogram was generated to assist in correlating these data. Seismic attributes were applied to enhance seismic data interpretation, revealing key geological features. This study focuses on verifying two potential gas anomalies. The first anomaly involves structural attributes, such as discontinuity and fault likelihood, crucial for detecting fault systems and assessing gas leakage. Fault sealing properties, whether fully sealed, partially sealed, or non-sealed, are important for understanding gas accumulation and migration. The second anomaly concerns stratigraphic attributes, using three types: sweetness, reflection strength, and spectral decomposition. Sweetness and reflection strength are effective for identifying gas, highlighting zones with high reflectivity and hydrocarbon presence. Spectral decomposition is particularly valuable for delineating channel fairways, identifying channelized gas-bearing sands, and clarifying the Pliocene anomaly, which indicates prime drilling and development locations. This study integrates 3D reprocessed seismic data from 2018 and well data, providing a comprehensive seismic interpretation that enhances understanding of gas reservoir characteristics.

Keywords: Seismic Attributes, gas reservoirs, Baltim Field, Nile Delta Channels

INTRODUCTION

The Nile Delta currently spans approximately 60,000 km^2, with around two-thirds of Egypt's gas production originating from this region. The estimated gas resource volume in the Nile Delta Basin is 223 trillion cubic feet (TCF), distributed across 126 gas deposits along the basin's rim (Kirschbaum et al., 2010), making it Egypt's most productive gas-producing area. Consequently, extensive research has been conducted to understand the region's structural framework, stratigraphy, and reservoir types, improving models and enhancing exploration success. Although reservoirs across multiple stratigraphic layers produce hydrocarbons, the Lower Pliocene shows a unique seismic response compared to the Late Miocene and Early to Late Pliocene sections.

The term "Baltim field" refers to three distinct gas fields within the Nile Delta (Abd El-Gawad et al., 2019; Abdel-Fattah et al., 2023; Hesham et al., 2023; Kadi et al., 2020; Sarhan, 2021a, b; Sarhan, 2022; Eid et al., 2024). Located in the northern Nile Delta, between 31°42'21.71" N, 31°59'07.22" N and 31°6'42.55" E, 31°16'49.42" E, the Baltim fields sit approximately 15 km offshore, occupying the northern portion of the Abu Madi Paleo-valley

© The Author(s). 2024 **Open access** This article is distributed under the terms of the Creative Commons Attribution 4.0 International License (https://creativecommons.org/licenses/by/4.0/), which permits unrestricted use, distribution, and reproduction in any medium, provided you give appropriate credit to the original author(s) and source, provide a link to the Creative Commons license, and indicate if changes were made.

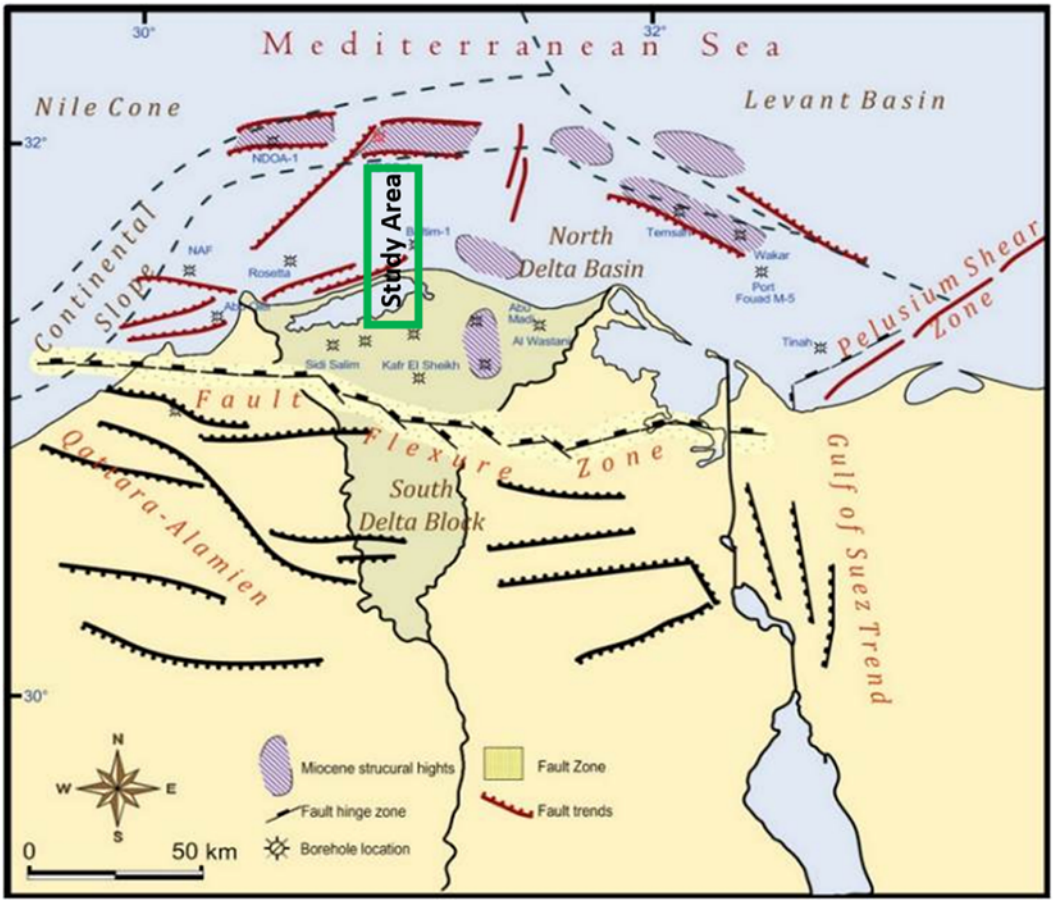

Fig. 1. Nile Delta subsurface main structure (Makled et al., 2017)

(Fig. 1). Water depths range between 45 to 60 m, and recent discoveries, particularly the 2015 Zohr field, have positioned the Eastern Mediterranean as a key area for gas exploration (El-Gendy et al., 2023).

The Baltim field spans approximately 30 km in length and 5 km in width, as depicted in Fig. 2a. This study focuses on the Baltim North concession, using data from five wells: two orange wells for the first Pleistocene anomaly and three green wells for the Pliocene anomaly (Fig. 2b).

A seismic "bright spot" is an intense amplitude anomaly that stands out within the seismic context, often indicating gas accumulation within terrigenous sand reservoirs (Sarhan, 2017). These bright spots typically highlight gas reservoir boundaries and gas-water contacts, if present, due to high reflection coefficients caused by low seismic velocities and gas densities, or occasionally light oil. High-brightness regions often appear in the shallower portions of seismic sections within recent sediment sequences.

In the Baltim area, the Kanaria prospect contains two main targets: the first in the Pleistocene, with dimensions of approximately 2,403 m by 2,168 m (area: 5,209 m²), and the second in the Pliocene, covering 5,488 m² with dimensions of 4,012 m by 1,368 m. These two prospects are bisected by a SW-NE fault, creating a four-way dip closure. The amplitude map, extracted from the reservoir's top, shows that the Pleistocene prospect is primarily stratigraphic, while the Pliocene prospect is structurally controlled and separated by a minor fault with a 30 m throw.

Seismic attributes are measurements derived from seismic data (Zelenika et al., 2018) and typically include time, amplitude, frequency, and attenuation. These attributes can be classified into two categories: time-based attributes, which are associated with structural features, and amplitude-based attributes, which are primarily used to characterize reservoirs and analyze stratigraphy. This study identifies the most effective seismic attributes for detecting hidden channels, including RMS amplitude,

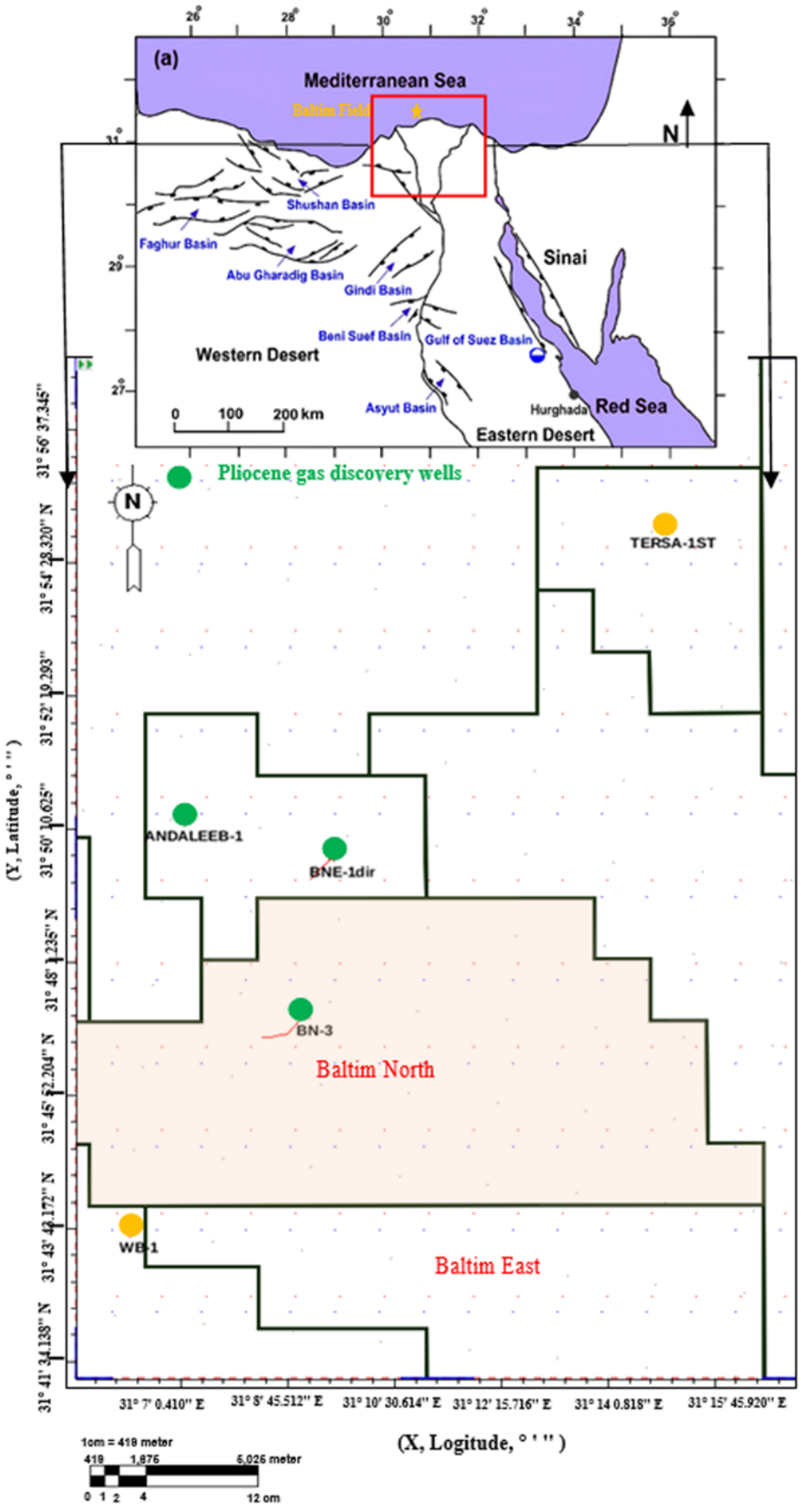

Fig. 2. a). A regional map displays the position of Baltim Field with the locations of several gas fields within the offshore portion of the Nile Delta Basin (adapted after El-Fawal et al., 2016b. b). Location map of Baltim field with 3D post-stack time migration (PSTM), defined as Del central reprocessing seismic time migration

envelope, sweetness, reflection strength, and spectral decomposition (Ghosh et al., 2010). These attributes are particularly useful for mapping the distribution of sand in the fairways of Pleistocene and Pliocene reservoirs.

The integration of structural and amplitude maps enhances the identification of reservoirs in the study area. Additionally, incorporating attributes related to structural dip and discontinuity improves the visual representation of seismic sections, providing clearer identification of both prominent and subtle faults. In particular, the discontinuity attribute plays a critical role in interpreting structural discontinuities and fault delineation, as it is sensitive to channel shapes (Chopra and Marfurt, 2007)

Confirming the existence of gas sand is challenging, particularly given the small amounts of gas that appear at far amplitude with noticeable brightness compared to near amplitude, as described in Class III of Amplitude versus Offset AVO classes (El-Ata et al., 2023; Koson et al., 2021). Traditional methods of seismic interpretation often led to confusion regarding the distinction between small and large gas accumulations, especially after identifying gas-bearing sand horizons. In this study, we utilize depth structure maps overlaid with far and near amplitude maps, revealing that the far amplitude exhibits a significantly higher magnitude than the near amplitude. This characteristic is indicative of Class 3 AVO behavior, suggesting substantial hydrocarbon potential.

The integration of seismic attributes is crucial for enhancing the understanding of hydrocarbon potential during structural interpretation. Discontinuity and fault likelihood attributes reveal fault trends, while stratigraphic attributes, such as sweetness and reflection strength, provide further analytical support. Additionally, spectral decomposition, based primarily on frequency-domain analysis, effectively illustrates channel orientations. These attributes facilitate the identification of gas anomalies in the Kafr El-Sheikh and El-Wastani Formations from the Pleistocene period, where the reservoirs consist of stacked channels ranging from 42.5 to 54 km in length. Along with quantitative seismic attributes, qualitative interpretations of structural patterns and reservoir characteristics are essential for improving our understanding of hydrocarbon potential.

This study recommends drilling both the El Wastani prospect, which covers an area of approximately 5,209 m² (with dimensions of 2,403 m in length and 2,168 m in width), and the second Pliocene prospect, covering approximately 5,488 m² (with dimensions of 4,012 m in length and 1,368 m in width), to explore these anomalies as prospective targets. Seismic characteristics play a crucial role in highlighting and differentiating predictive features, serving as indicators of hydrocarbon presence or absence. In petroleum exploration and reservoir evaluation, seismic attributes are used to accurately map subsurface geological formations, analyze seismic data, and gain insights into reservoir properties.

The identification of channelized sand features within the Plio-Pleistocene succession of the Baltim concession was accomplished using a range of seismic attributes, including horizon amplitudes and spectral component decomposition. These attributes also helped to clarify the structural patterns in the study area, contributing valuable techniques and insights to the geoscientific community, with significant potential for application in both regional and international contexts.

The determination of channelized sand features within the Plio-Pleistocene Succession of the Baltim concession was achieved using a diverse range of seismic attributes, including horizon amplitudes and spectral component decomposition. These seismic attributes also helped to illustrate the structural patterns in the research field, contributing original techniques and findings to the geoscientific community with significant potential for adaptation in both regional and international contexts.

GEOLOGIC SETTING OF NILE DELTA

General stratigraphy

The stratigraphy of the Nile Delta's subsurface is shown in Fig. 3. According to El-Ella (1990), the Pliocene cycle, as described by Rizzini et al. (1978), is divided into two formations: the Kafr El-Sheikh and El Wastani. The early Pliocene deep-marine sequence of the Nile Delta was

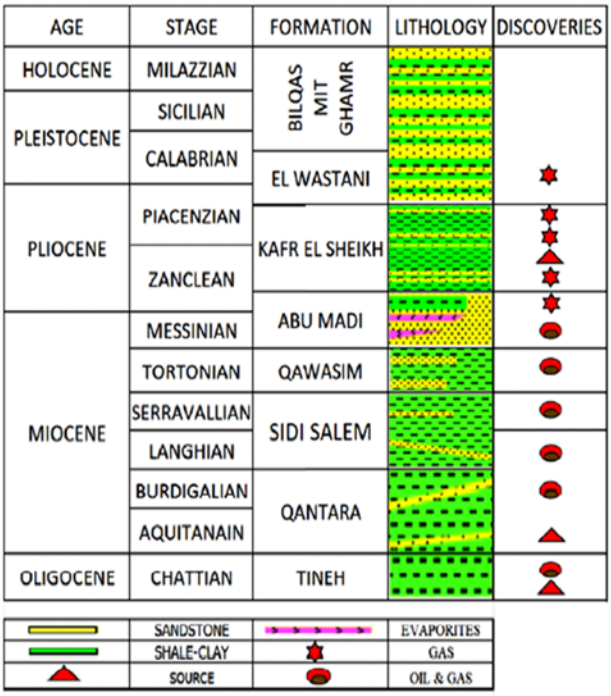

Fig. 3. Nile delta stratigraphic sequence (adapted from Kamel et al., 1998).

deposited unconformably over the "fluvio-marine" Abu Maadi and Qawasim Formations in the central subbasin, as well as the Rosetta "evaporative" strata in the eastern subbasin. The shale-bearing Kafr El-Sheikh Formation represents the marine sequences, with the formation's upper layers transitioning into river and coastal sands, which are classified as the El Wastani Formation, constituting the upper Pliocene cycle.

The Pleistocene/Holocene transgression cycle, represented by the Mit Ghamr and Bilqas Formations, directly overlies the Pliocene cycle. The stratigraphic nomenclature used here is based on the work of Rizzini et al. (1978), with the formations listed in chronological order from older to younger.

Kafr El-Sheikh Formation: The first unit of the Pliocene-Pleistocene cycle is the Kafr El Sheikh Formation, which is well-developed in many Nile Delta wells. The type section for this formation is located in well Kafr El Sheikh-1, where it is encountered between depths of approximately 1,277 and 2,735 m. The thick sand layers of the overlying El Wastani Formation, containing littoral fossils, mark the upper boundary of the Kafr El Sheikh Formation (Rizzini et al., 1978). The Kafr El Sheikh Formation was deposited during a transgressive event associated with a global rise in sea level (Sestini, 1989). A notable lithostratigraphic gap exists between the Kafr El Sheikh and the underlying Abu Madi and Qawasim (Rosetta) Formations.

El Wastani Formation: The El Wastani Formation is composed of thick sand beds interbedded with thinner clay layers, which progressively thin toward the upper part of the formation. This formation acts as a transitional zone, connecting the underlying Kafr El Sheikh Formation (Pleistocene-Holocene) with the coastal and continental sands of the overlying Mit Ghamr Formation (Kamel et al., 1998). It is recorded at Well El Wastani-1, where the rock unit has been drilled between -1,009 and -1,132 m True Vertical Depth Sub Sea (TVDSS). The formation was deposited in settings that were intermediate between the coastal to continental facies of the overlying Mit Ghamr Formation and the outer shelf conditions of the underlying Kafr El Sheikh Formation. The El Wastani Formation is characterized by intercalations of sandstone and shale strata.

The shale encountered in the Baltim-North 3 well is dark gray, occasionally greenish gray, blocky to sub-blocky, soft to fairly firm, silty to extremely silty, occasionally grading to siltstone, rarely sandy, and moderately dolomitic.

Structural setting

The Nile Delta is currently in a finely balanced condition on the precipice of the African tectonic plate's northernmost point. Since the Nile Delta resembles a triangle or lotus bloom from above, it is shown as an aberrant delta, or arc-shaped delta. The hydrocarbon potential of the Nile Delta sedimentary sequence is primarily associated with the Neogene strata, which are trapped against over-tilted fault blocks or listric fault planes (Barakat and Dominik, 2010; Barakat, 2010).

The Nile Delta itself resembles a triangular shape, with Cairo marking the apex, as described by Aal et al. (2000). These authors carefully analyzed the tectonic processes that shaped the Nile Delta basin, which developed through three main tectonic phases:

I. *Carboniferous to Late Cretaceous:* The

region was part of the North African passive margin, situated on the southern edge of the Tethys Ocean.

II. *Campanian to Late Eocene:* The area became a foreland basin under the influence of Alpine tectonics, resulting from the northward collision of Africa with Eurasia.

III. *Oligocene to Present:* The Nile Delta Hinge Zone became part of the transform margin associated with the oblique separation of the African and Arabian plates, which led to the formation of the Gulf of Suez and the Red Sea (Aal et al., 2000).

The current structure of the Nile Delta is a result of the complex interaction between four primary fault trends (Fig. 1):

-*Hinge Zone:* Located around 31° N, the Hinge Zone represents a significant area of flexure, separating the South Delta Massif from the northern portion of the Delta basin. This fault trend runs roughly east to west and exhibits considerable northward displacement, creating a divide between the North Delta and South Delta blocks.

-*Temsah Trend:* The Misfaq-Bardawil (Temsah) fault trend consists of a series of parallel NW-SE faults, with eastward throws. During the Middle Miocene, this trend was subject to right-lateral oblique slip movement.

-*Qattara-Eratosthenes (Rosetta) Trend*: This fault system, which trends NW-SW, exhibits significant structural relief due to translational displacement along the Qattara-Eratosthenes direction. This movement is associated with the Late Cretaceous period, as demonstrated by the overlying source rock layers from the Late Cretaceous to Early Tertiary deep-sea deposits. The fault system remained active from the early Miocene to the late Pleistocene, connecting the northern Delta basin with the southern Delta Block.

-*Baltim Trend* is a series of N-S trending faults that formed during the Late Eocene to present. This fault system likely resulted from the rejuvenation of pre-Tertiary structures during the Early Miocene.

DATA AND METHODOLOGY

Seismic Data and Grid Layout: The seismic data for this study is organized in a grid layout, covering three-dimensional offshore locations within the Baltim Concessions area. Five drilled wells were employed to align with this seismic grid, ensuring accurate integration between well and seismic data.

Seismic Data Quality and Limitations: The seismic dataset utilized for interpretation is of high quality, providing clear horizons and fault structures that facilitate detailed interpretation. However, a limitation arises near the shoreline, where recording conditions were challenging, resulting in areas with a lower signal-to-noise ratio. These low-quality areas, which are evident in some seismic sections and maps, presented potential challenges for accurate interpretation.
Handling Seismic Data Quality Limitations: To mitigate the effects of low signal-to-noise ratio, several processing techniques were employed to enhance data quality. Noise attenuation filters were applied to improve signal clarity in the affected areas, allowing for better identification of geological features. Additionally, amplitude normalization was carried out to minimize distortions caused by noise and to ensure consistent interpretation across the dataset.
Where necessary, additional seismic attributes, such as sweetness and fault likelihood, were utilized to strengthen interpretations in regions with lower data quality. These attributes are less sensitive to noise and help provide complementary insights into the subsurface, especially in areas where conventional methods may struggle. Manual interpretation adjustments were also made in the most challenging areas, using geological constraints and well data to refine interpretations in regions with lower seismic clarity. This multi-faceted approach helped address the data limitations and ensured the integrity of the seismic interpretation across the study area.

Seismic Interpretation: Seismic interpretation, including horizon and fault mapping, as well as the analysis of various seismic attributes, was performed using Landmark G&G DSG 10ep software. Seismic data for this study is organized in a grid layout, covering three-dimensional offshore locations within the

Baltim Concessions area. Five drilled wells were employed to align with this seismic grid, ensuring accurate integration between well and seismic data. Seismic-to-well tie and wedge modeling were carried out using Petrel software, which helped assess vertical resolution and further refine the interpretation.

Seismic Attribute Selection and Spectral Decomposition: To enhance the interpretative accuracy, especially in areas with low signal-to-noise ratios, spectral decomposition was applied alongside other seismic attributes. Spectral decomposition analyzes the frequency components of seismic data, enabling the identification of subtle lithological features and channelized gas-bearing sands. This technique is particularly useful for resolving thin beds of sand layers, which are more visible at higher frequencies, and it helped clarify the Pliocene channel fairway and gas-bearing sands in regions affected by lower signal-to-noise ratios. Along with spectral decomposition, sweetness and fault likelihood were selected as key seismic attributes due to their relevance to the geological context of the Nile Delta. Sweetness is effective at distinguishing lithology and highlighting gas-bearing formations by combining amplitude and frequency characteristics to emphasize softer rock layers commonly associated with hydrocarbon presence. This attribute is especially suited for detecting gas-saturated zones in the Baltim area. Fault likelihood, on the other hand, was chosen for its ability to delineate fault structures, which are crucial for understanding the region's tectonic history and reservoir characteristics. It enhances fault visualization, essential for assessing the compartmentalization of the reservoir, a key factor in resource estimation and development. Together, these seismic attributes were integrated to provide a comprehensive analysis of the geological and structural complexities of the study area.

Seismic Interpretation Software: Seismic interpretation, including horizon and fault mapping and analysis of various seismic attributes, was performed using Landmark G&G DSG 10ep software. Seismic-to-well tie and wedge modeling were carried out using Petrel software, which helped assess vertical resolution and further refine the interpretation.

Workflow

The approach starts by examining the well logs that are currently accessible for the chosen Wb-1 well for the first Pleistocene anomaly and the BNE-1 well for the second anomaly. Several well-log analyses using gamma ray, resistivity, and Vp sonic logs are utilized to detect the reservoir intervals.

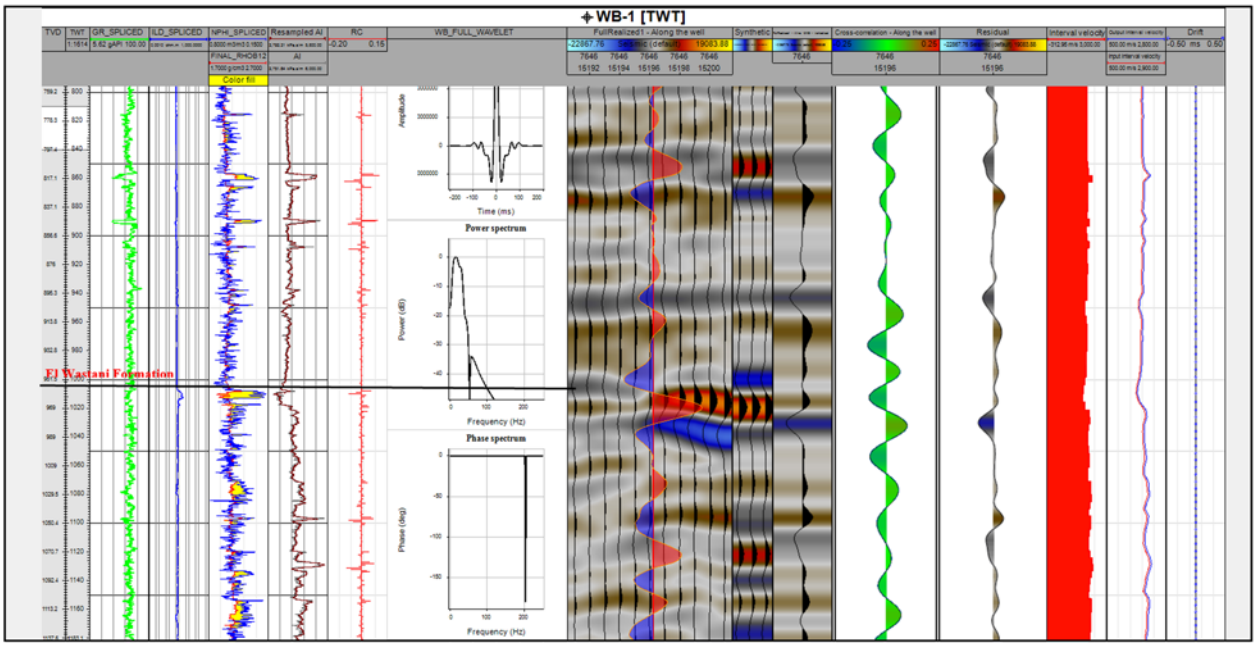

Fig. 4. A synthetic seismogram for WB-1 well, generated using the sonic and density logs, is included, which shows a good match between the synthetic seismogram and the original full post-stack seismic section

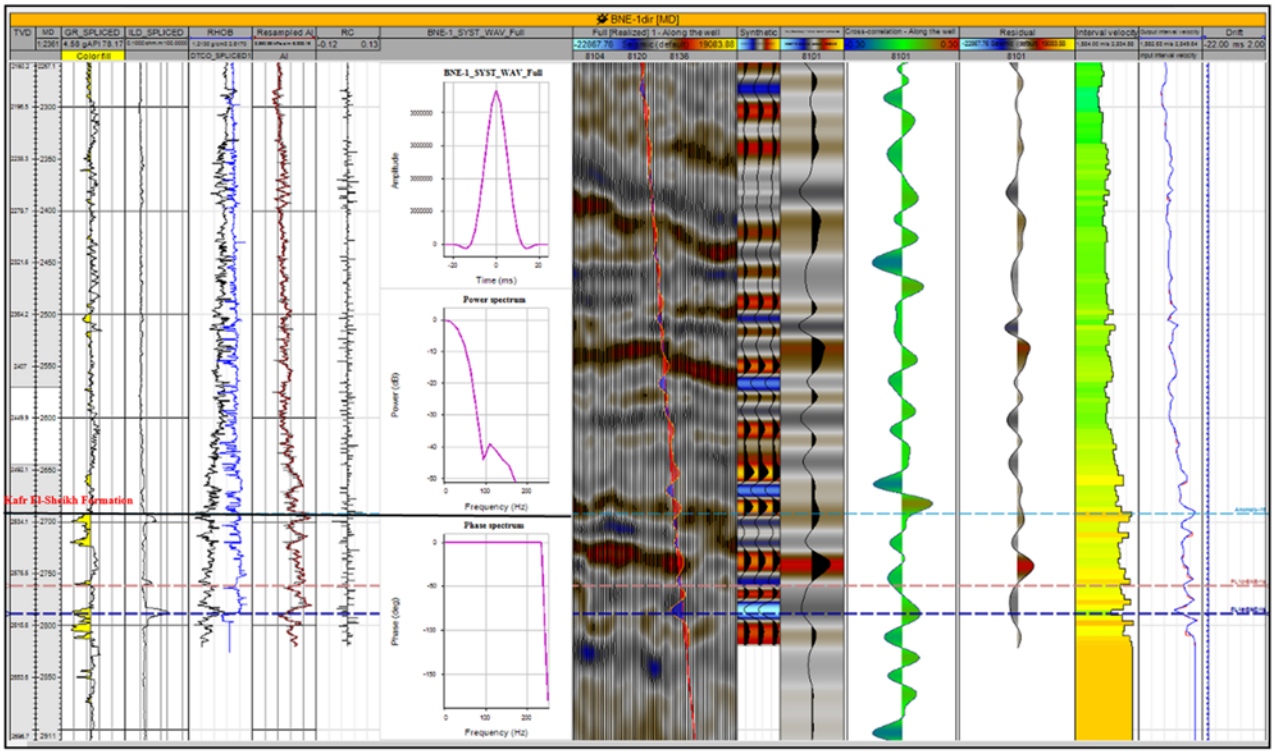

Fig. 5. Synthetic seismogram for BNE-1 well, generated using the sonic and density logs, is included, which shows a good match between the synthetic seismogram and the original full post-stack seismic section

Seismic to well tie:

The well-to-seismic tie is a valuable method for accurately identifying and interpreting drilled anomalies within the seismic data (Amer et al., 2023; Barakat et al., 2019; Eid et al., 2023; Noureldin et al., 2023). This method relies on density and velocity data (Amer et al., 2024; Eid et al., 2024; El-Sayed et al., 2024; Lasheen, et al., 2024; Mohamed et al., 2024), frequently collected along the borehole using (Amer et al., 2024; Eid et al., 2024; El-Sayed et al., 2024; Lasheen, et al., 2024; Mohamed et al., 2024) wireline logging tools. Vertical resolution from wireline logs is higher than that of seismic data, offering a more precise synthetic representation. To generate a synthetic seismic trace, the reflection coefficients are convolved with a seismic wavelet (Veeken, 2007). The synthetic seismogram must match the actual seismic data's polarity and wavelet form (Alotaibi and Metwally, 2024; Ewing, 2001; Barakat, 2010; El-Sayed et al., 2024; Lasheen, et al., 2024). The seismic data used in this study has European polarity with zero phase, where a trough indicates an increase in acoustic impedance.

The first anomaly, located in well Wb-1, corresponds to the Pleistocene layer (Fig. 4), while the second anomaly, identified in the BNE-1 well, occurs in the Pliocene layer (Fig. 5).

Wedge model: The objective of wedge modeling is to determine the optimal thickness of a thin reservoir layer to avoid misinterpretation during seismic analysis (Abdulkareem, 2022). While strong amplitudes typically indicate changes in acoustic impedance that are associated with gas accumulation, the reservoir thickness must exceed a quarter of the seismic wavelength to ensure accurate interpretation. This thickness ensures that the seismic resolution is sufficient to avoid destructive interference (when the peak coincides with the trough) and constructive interference (which causes exaggerated peaks). Tuning effects occur in thin layers, with the amplitude increasing as the layer thickens. If the reservoir layer is thinner than the amplitude thickness, the amplitude will decrease, marking the limit of seismic visibility (Fig. 6a).

For this study, the wedge model was applied using Petrel software on the BNE-1 direction well. The isochron thickness was extracted by relating the isochron thickness to the average magnitude (Fig. 6b). Wedge model equations

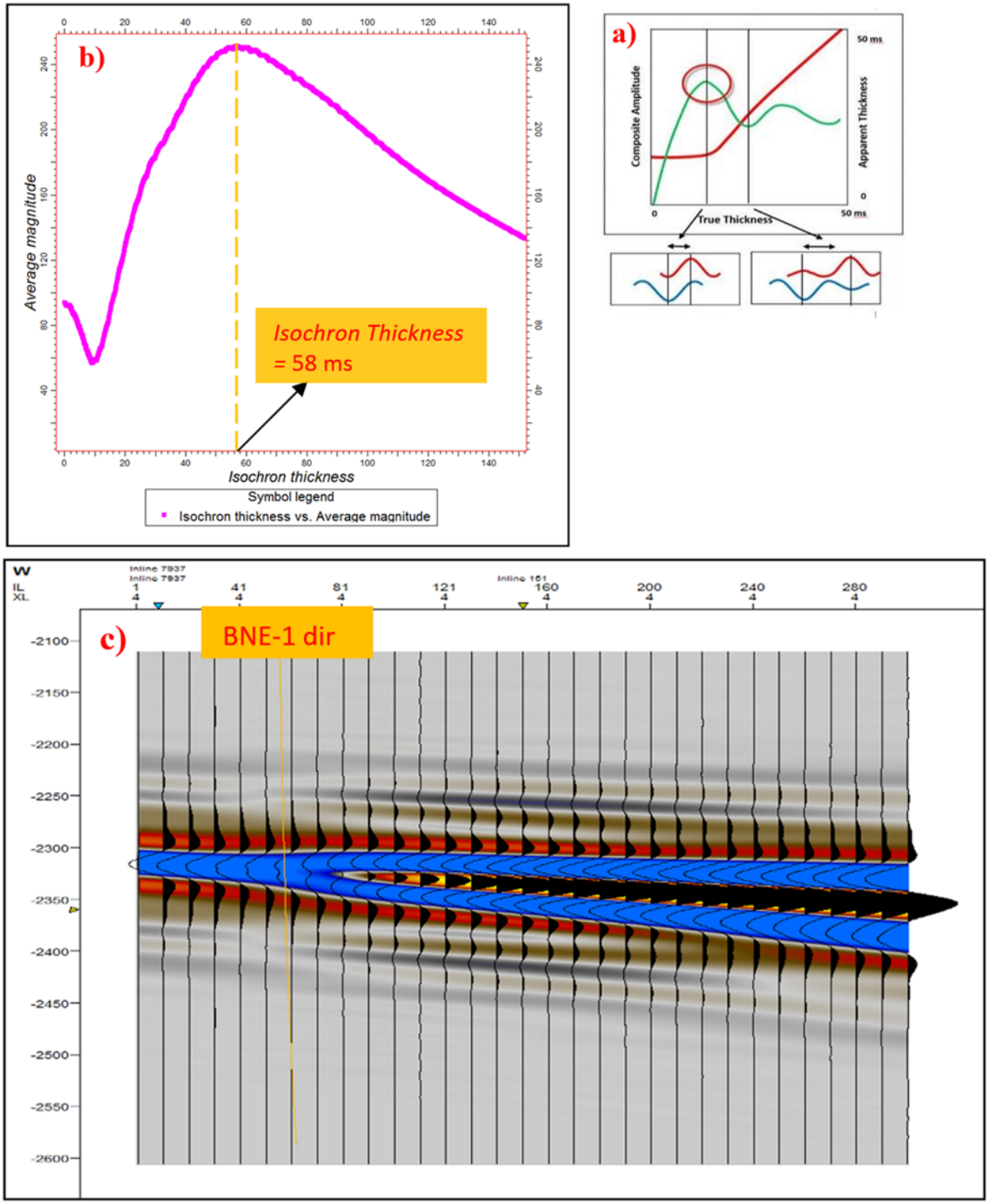

Fig. 6. a) Amplitude Versus Thickness and Concept of Tuning. b) Relation between Isochron thickness and the average magnitude of BNE-1 dir well. c) Wedge model of BNE-1 dir well.

were then applied to generate the wedge model for the BNE-1 direction well (Fig. 6c). The tuning thickness was determined to be 30 m. Below this depth, distinguishing the anomaly or interpreting the gas-sand horizon becomes challenging. As such, seismic attributes play a crucial role in confirming the presence of gas within both prospective anomalies.

Seismic attributes

In hydrocarbon exploration, successful hydrocarbon identification begins with a good understanding of subsurface seismic data (Amer et al., 2023; El Hameedy et al., 2023; Mahmoud et al., 2023). This facilitates the identification of the seismic data's initial processing step by direct measurement, logical reasoning, or

experience-based reasoning (Ibekwe et al., 2023).

Seismic attributes are characterized as the most informative tools to characterize seismic features, such as layer velocity, acoustic impedance inversion (Abdel-Fattah and Tawfik, 2015; Farfour et al., 2021; Oumarou et al., 2021; Ibekwe et al., 2023; Sarhan and Safa, 2017), and pore pressure prediction (Pwavodi et al., 2023), after the emergence of intricate trace theory during the earlier phases of the 1970s, the initial application of seismic attribute analysis was directed towards the realm of oil exploration in the decades between the 1970s and 1980s (Sheriff, 1994), the term "attributes" pertains to measurements that are generated from seismic data, for instance, envelope amplitude (commonly referred to as "reflection strength"), velocity, instantaneous frequency, polarity, instantaneous phase, slope, slope azimuth, seismic interpretation methods have made it conceivable to calculate volumes of structural attributes and augment faults in seismic data due to automated fault extraction using a variety of seismic features (Imran et al., 2021). Semblance, coherency, and the uninterrupted nature of seismic reflections can be computed by considering other attributes, whereas variance and other attributes quantify the discontinuity.

Seismic attributes pertain to metrics that capture precise geometric, statistical, or cinematographic characteristics deduced from seismic information (Chen and Sidney, 1997). All seismic parameters can be categorized as seismic attributes using the seismic waveform's amplitude, shape, and position. 3D seismic properties aid in the extraction of useful information (Coren et al., 2001). The interpretation of channels, the fluvial system, carbonate deposits, marine turbidity, and other potential and depositional settings is conducted using these fundamental criteria (Chopra and Marfurt, 2005b; Naseer et al., 2022; El-Ella, 1990).

Additionally, it encompasses various quantifications that make use of seismic data; including orientation, polarity, and envelope, dips direction, instantaneous phase, and instantaneous frequency. It is vital to highlight that attribute analysis complements traditional structural interpretation and allows rigorous evaluation of the particular properties of a given attribute (Nissen, 2002).

Seismic attributes can be categorized as two distinct types of attributes. The first type is a structural seismic attribute, which is used mainly to recognize faults, and the other type is a stratigraphic attribute, which is used mainly to identify channel features and unconformities. All of these seismic characteristics are a good tool for indicating bright spots (hydrocarbon indicators) and for the declaration of various Pleistocene and Pliocene channels.

Structural attributes

Discontinuity: The discontinuity attribute is a post-stack measurement used to determine the similarity or difference of seismic traces locally. It evaluates the lateral continuity of seismic reflectors and assesses how similar a single trace or set of traces is to its surroundings (Chopra and Marfurt, 2007; Kington, 2015). Discontinuity is an important characteristic used to define geological features such as deltas, faults, and undersea canyons. Additionally, coherency is useful for identifying features like beaches and deltas, as it measures how similar waveforms or traces are to one another (Almasgari et al., 2020). The most widely used seismic qualities are intrinsic structure-based coherence, apparent coherence, and other dissimilarity properties.

Fault Likelihood: It is a post-stack seismic attribute designed to detect faults by identifying discontinuities or crosscutting seismic reflectors. This attribute integrates multiple variables to improve fault detection accuracy (Hale, 2013; Lou et al., 2019). Advances in fault likelihood analysis have made it possible to automatically extract faults from seismic data with greater clarity and precision. When used alongside manual fault interpretation, FLH can expedite the process of large-scale structural interpretation in exploration contexts by providing a comprehensive fault map (Harris et al., 2019). Fault likelihood is expressed as a value between 0 and 1, where higher values indicate a stronger likelihood of fault presence.

Stratigraphic attributes

RMS Amplitude: Seismic amplitude, a post-stack property, is important for determining the lithology, geometry, and depositional context of sedimentary structures. An assessment of the discrepancy in qualities between two layers is seismic amplitude. According to several authors (Okocha and Atakpo, 2017; Hart, 2008), hydrocarbons, particularly gas sand, cause amplitude brightening in tertiary clastics. Seismic amplitude has been the most widely utilized characteristic for identifying reservoirs (El-Saoud et al., 2022; Emujakporue and Enyenihi, 2020).

Sweetness: The sweetness is a helpful tool for seismic attributes for accurately depicting the depositional environment, quality of reservoir, and Litho-facies differentiation (Zelenika et al., 2018). The definition relies on the observation that sweet spots in young, unconsolidated sediments are frequently distinguished by seismic features of high amplitude and low frequency (El-Nikhely et al., 2022; Hossain, 2019), according to Equation 1, sweetness *s(t)* is calculated by trace envelope *a(t)* divided by the square root of the average frequency *fa(t)*,

$$s(t) = \frac{a(t)}{\sqrt{fa(t)}}$$

The amplitude response of an envelope, and its value at its apex. Sweetness, on the other hand, is utilized in a *variety* of ways (Oliveros and Radovich, 1997). For instance, it is employed to illustrate the geometry of a plan-form turbidity channel. Additionally, its purpose extends to the identification of "sweet spots," which are locations that exhibit proclivity for oil and gas.

Reflection Strength

Most of the non-massive unit demonstrates diminished reflection strength, or a faint blue color, as per the envelope attribute (Sarhan, 2017), which signifies acoustically robust (luminous) occurrences for pessimistic and optimistic incidents and serves as the most prevalent track characteristic. It is derived from intricate seismic signal trajectories and is utilized to accentuate pivotal seismic aspects. The envelope symbolizes that the reflection coefficient is closely correlated with the signal's momentary power and magnitude. This casing is appropriate for accentuating disparities, alterations in lithology, faults, and other similar phenomena.

Sedimentary modifications, repercussions of adaptation, and demarcations of sequences. The bright spots of this characteristic hold significance as they can serve as an indication of a gas presence, particularly in relatively recent clastic deposits. This property possesses the benefit of remaining unaffected by seismic data phase or polarity, which both alter the apparent brightness of the reflections. This is in contrast to raw seismic trace values. The sand layers or channel bodies that appear bright are most likely caused by a difference in acoustic impedance. Lateral discontinuous characteristics are typically used to identify faults in the envelope attribute.

The seismic feature, however, is challenging to observe (Azeem et al., 2015). To put it simply, reflection strength is the overall seismic trace envelope for each sample of time and illustrated by is the following Equation 2.

$$Reflection\ Strength = \sqrt{(Real\ traces)^2 + quadrature\ reflection}$$

Spectral Decomposition: It is a technique that links user-defined cosine frequencies with the autocorrelation function of raw seismic data (Akinwale et al., 2022; Laughlin et al., 2002; Ismail et al., 2020). This method can reveal subtle lithological features that may not be apparent in the original amplitude data and help identify potential areas of hydrocarbon enrichment. It is also effective for characterizing sedimentary structures. For example, spectral decomposition can be used to analyze incised valleys (Peyton et al., 1998) and detect low-frequency shadows beneath oil reservoirs through the matching pursuit decomposition approach (Castagna et al., 2003). By converting seismic data into frequency components, spectral decomposition enables the identification of low-frequency features that may indicate the presence of hydrocarbons (Chopra and Marfurt, 2007).

Seismic data responds uniquely to different frequencies. Higher frequencies, for instance, result in shorter wavelengths that can detect narrower geological features, such as slender channels (McArdle and Ackers, 2012). The

spectral components reflect the geological characteristics of the subsurface, with varying thicknesses of channels and infill producing distinct spectral responses (Del Moro, 2012). The primary goal of spectral decomposition is to analyze the frequency composition of seismic data, rather than just the amplitude (Roshdy et al., 2022). This allows interpreters to evaluate multiple phase volumes and select the one that best represents a specific geomorphological feature or framework (Subrahmanyam and Rao, 2008).

In practical terms, spectral decomposition is particularly useful for resolving thin beds of sand layers. Thinner beds are more visible at higher frequencies, while thicker beds are better detected at lower frequencies. Spectral decomposition can be applied in both vertical and horizontal directions, providing valuable insights into the presence of hydrocarbon-bearing tidal channels (Noureldin et al., 2023).

RESULTS AND INTERPRETATION

Seismic attributes play a crucial role in confirming the presence of gas in prospective anomalies and in identifying the optimal locations for drilling. However, conventional seismic interpretation alone is limited in its ability to definitively confirm gas presence after correlating seismic data with well logs and determining the gas horizon for the identified anomalies. Well WB-1 is considered a key well for the first Pleistocene anomaly, while BN-3 is critical for the second Pliocene anomaly. Production at BN-3 commenced in October 2015 and is currently operating at an average rate of 40 million standard cubic feet per day (MMscf/d)

The first structural attribute critical for fault detection in the El Wastani and Kafr El-Sheikh formations is the discontinuity attribute, a post-stack feature. Areas with high coherence indicate continuous reflections and are represented in white, while areas with poor coherence, often indicating fault zones, appear in gray or black. As shown in Fig. 7 and Fig. 8, the main fault polygons are represented by black elements, highlighting the key fault zones in both the Pleistocene and Pliocene anomalies. In Fig. 9 and Fig. 10, the same maps are displayed with fault polygons in gray, illustrating the similarity between the two fault maps. Both sets demonstrate a consistent trend of the main SW-NE fault direction, further confirming the correlation between the fault structures in the Pleistocene and Pliocene anomalies.

The secondary structural attribute used for detecting faults in the El Wastani and Kafr

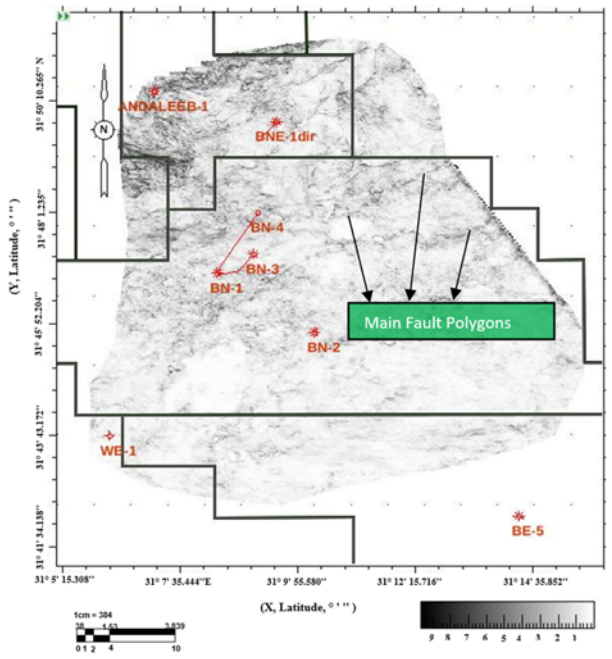

Fig. 7. Pleistocene discontinuity map, where fault polygons are represented by black color elements, highlighting the major faults in the Pleistocene anomaly

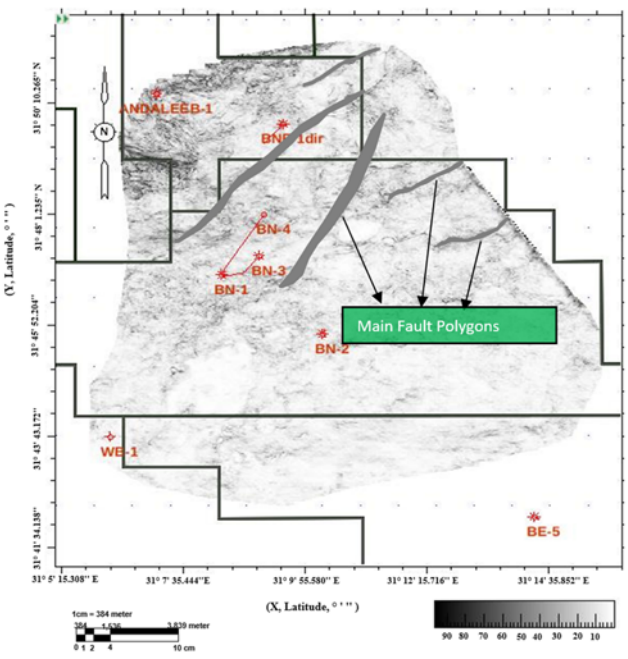

Fig. 8. Pleistocene discontinuity map, where fault polygons are represented by gray polygons, illustrating the fault zones and emphasizing the consistency of the fault trends

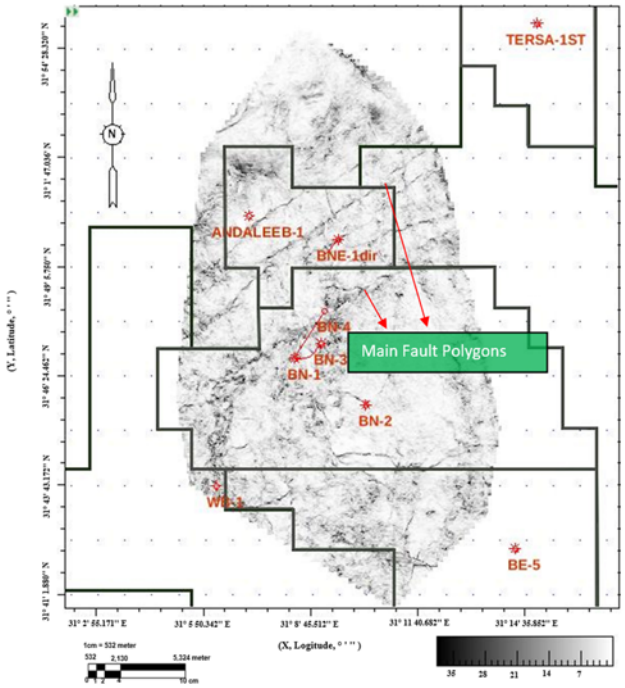

Fig. 9. Pliocene discontinuity map, where fault polygons are represented by black color elements, identifying the major faults in the Pliocene anomaly

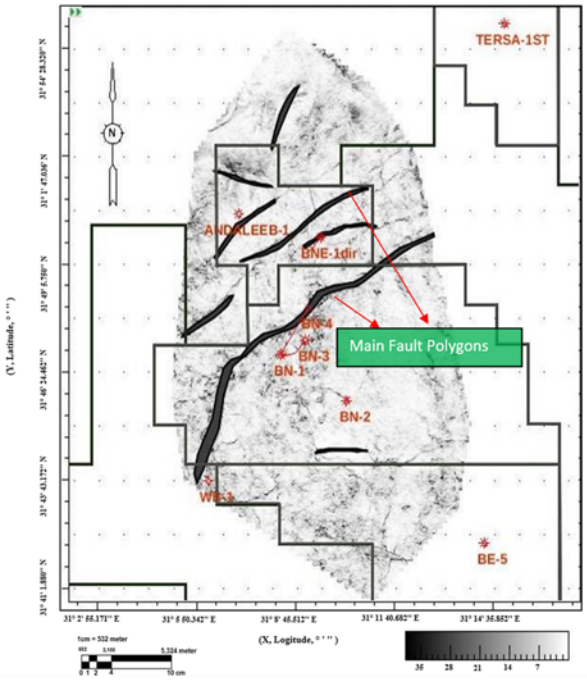

Fig. 10. Pliocene discontinuity map, where fault polygons are represented by gray polygons, showing the fault zones and confirming the SW-NE fault trend alignment across the anomaly

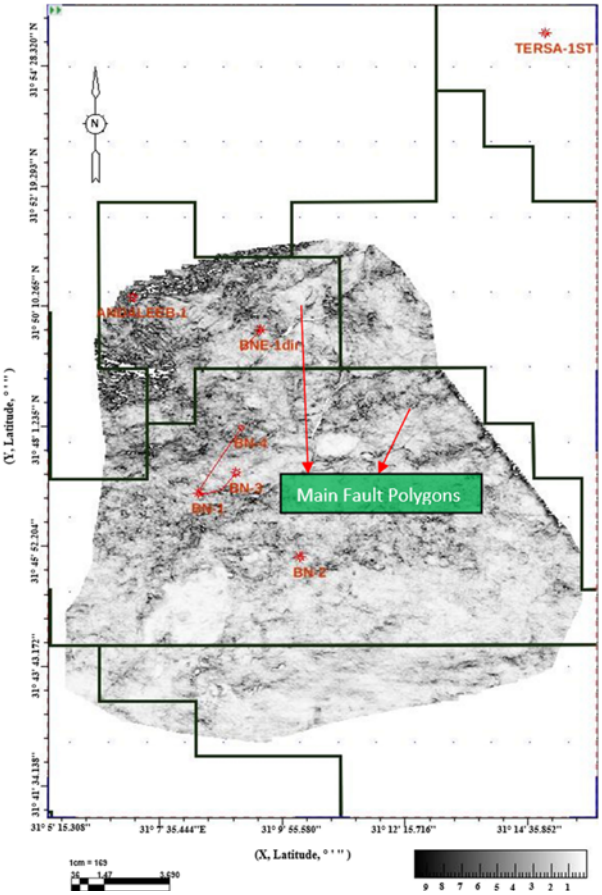

Fig. 11. Pleistocene Fault Likelihood (FLH) map, in which fault polygons are represented by black color elements

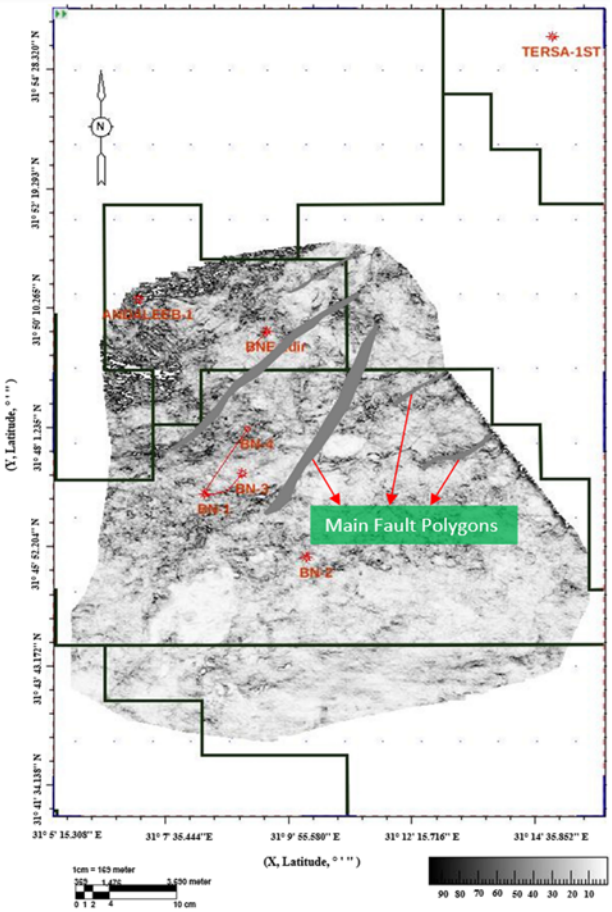

Fig. 12. Pleistocene Fault Likelihood (FLH) map, in which fault polygons are represented by gray polygons

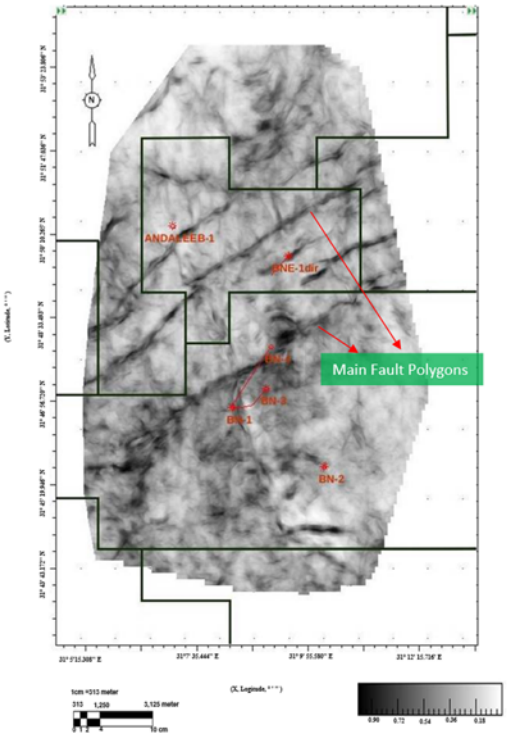

Fig. 13. Pliocene Fault Likelihood (FLH) map, in which fault polygons are represented by black color elements

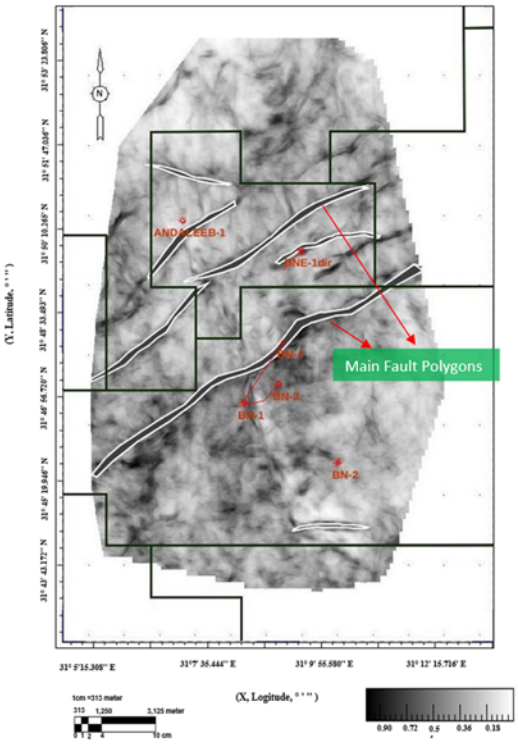

Fig. 14. Pliocene Fault Likelihood (FLH) map, in which fault polygons are represented by gray polygons

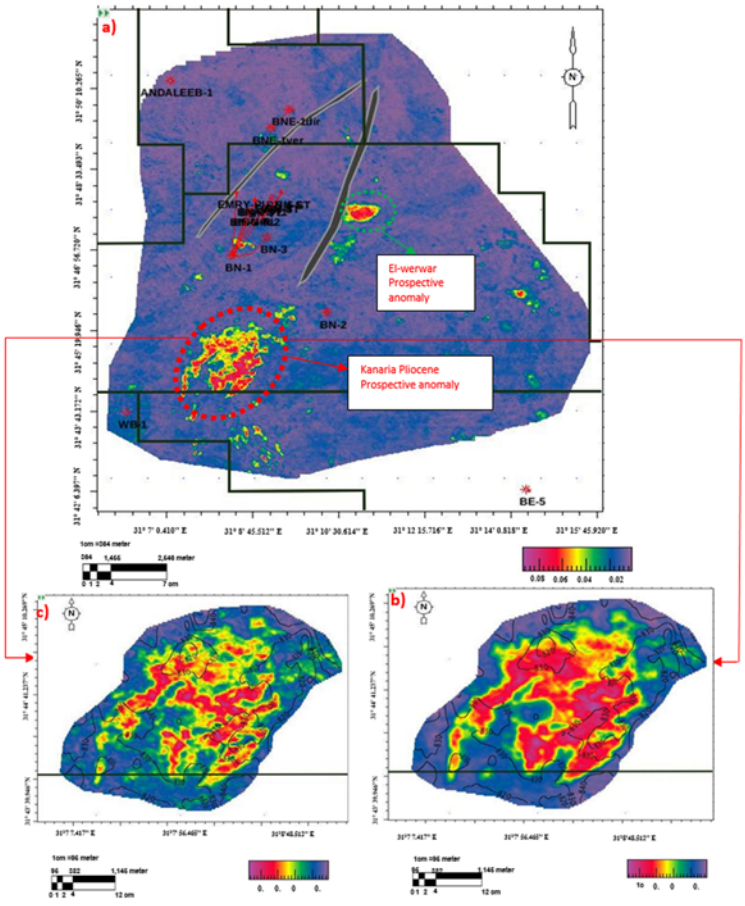

Fig. 15. a) Regional far amplitude map for Pleistocene Formation extracted at window (-25, 50) ms. b) Zoomed Far amplitude map for Pleistocene Prospect anomaly overlaid by depth structure contour map, extracted at window (-25, 50) ms. c) Zoomed Near amplitude map for Pleistocene Prospect anomaly overlaid by depth structure contour map, extracted at window (-25, 50) ms

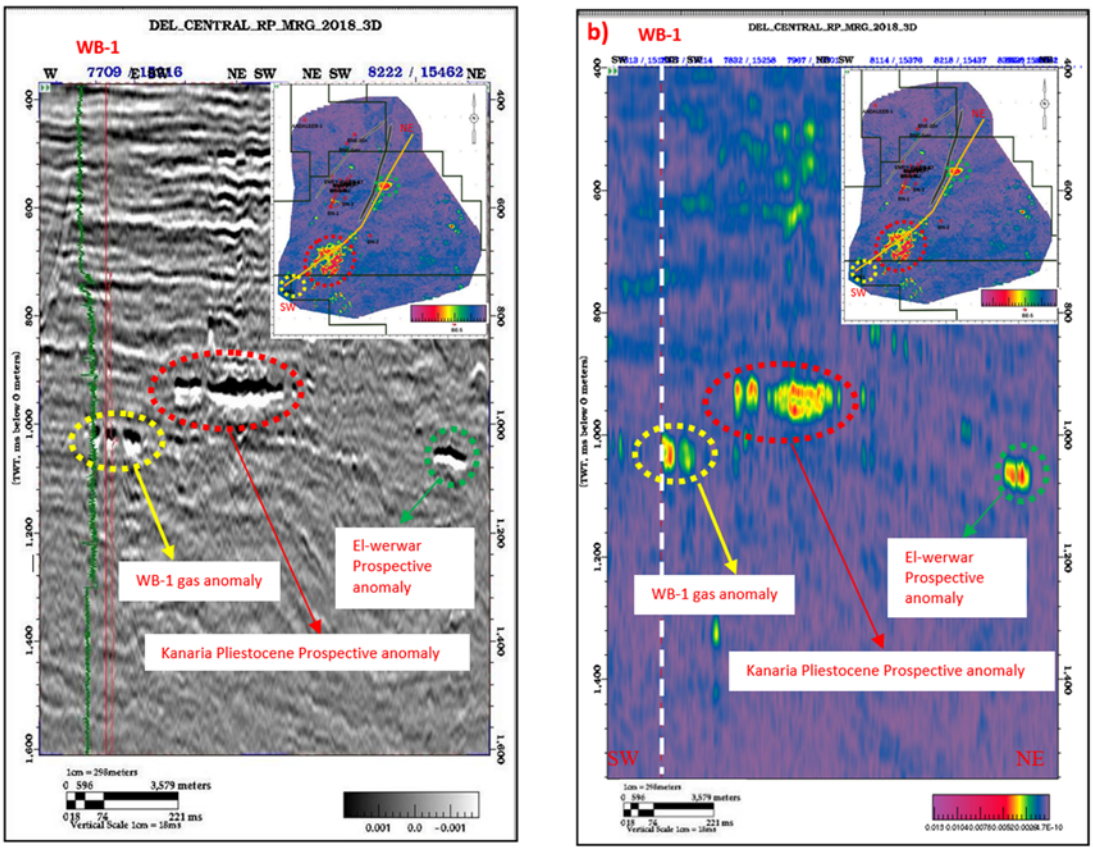

Fig. 16. a) SW-NE Seismic Section at full post-Stack Time Migration (PSTM), passing through WB-1 well and Kanaria Pleistocene Prospect. b) SW-NE Seismic Section at Far-Post-Stack Time Migration (PSTM), passing through WB-1 well and Kanaria Pleistocene Prospect

El-Sheikh formations is the fault likelihood attribute, which was specifically created to locate and record faults within the research area. The program scans a range of fault dips to identify the faults with the highest likelihood. Regions with high coherence, which indicate continuous reflections, are shown in white, while areas with low coherence, typically associated with fault zones, are represented in darker shades such as gray or black. As seen in the Fig. 11 and Fig. 12, the major fault zones are highlighted by black elements, marking the significant fault lines in both the Pleistocene and Pliocene formations. In the Fig. 13 and Fig. 14, similar maps are presented with fault polygons shown in gray, demonstrating the close correlation between the two fault maps. Both sets reveal a consistent trend of the main fault orientation along the SW-NE direction, reinforcing the connection between fault structures in the Pleistocene and Pliocene anomalies.

The second category of seismic attributes is known as stratigraphic attributes, which can be divided into four types. The first type, Root Mean Square (RMS) Amplitude, describes sand distribution across the outermost shelf or slope in the north, forming sand bars and channels. This distribution is evident in the amplitude maps of the Pliocene Kafr El-Sheikh and Pleistocene El Wastani formations. For the Pleistocene succession (El-Wastani horizon), regional extraction reveals the highest positive amplitude from far-angle stack seismic data (Fig. 15a). Far-amplitude produces higher amplitude and brightness than near-amplitude, corresponding to Class III of Amplitude versus Offset (AVO) classes (Fig. 15b-c).

The random seismic section (SW-NE), derived from far post-stack and RMS post-stack time migrations, passes through the discovery well WB-1 (yellow circle) and identifies two main prospects. The Kanaria prospect is marked by a red circle and the El-Werwar prospect by a green circle (Fig. 16a-b). During the Pliocene succession, the maximum positive amplitude, recorded from the far-angle stack between 10 m above and 40 m below the Kafr El-Sheikh horizon, again displays higher brightness in far-

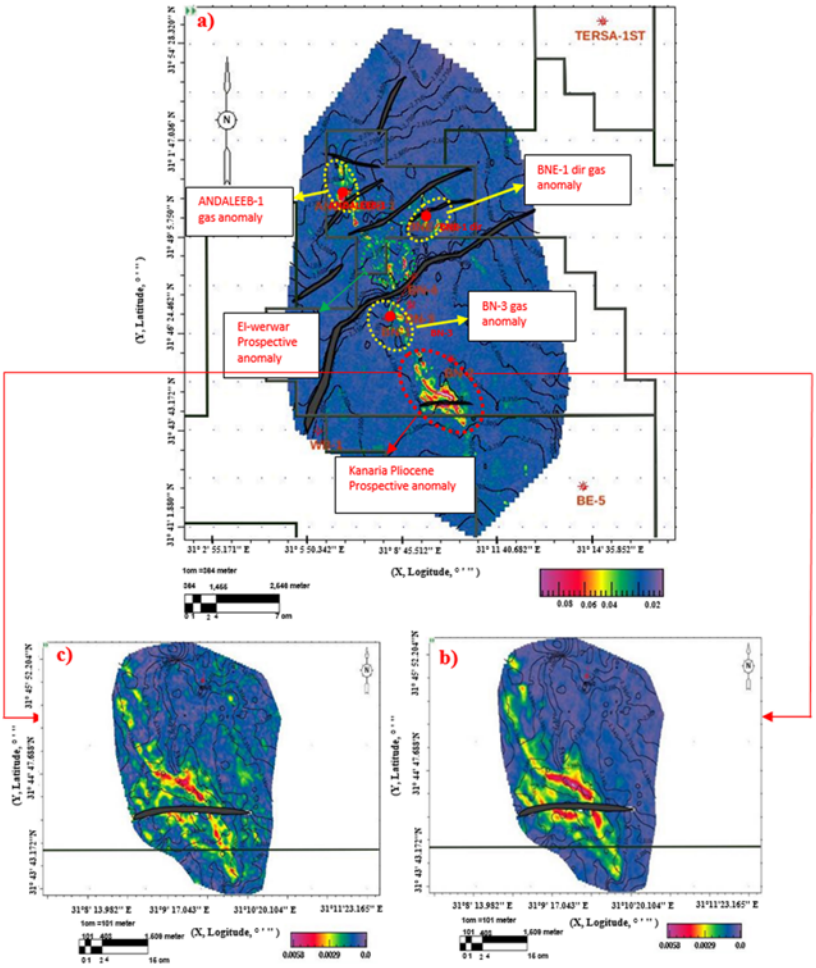

Fig. 17. a) Regional far amplitude map for Pliocene Formation extracted at window (-10, 40) ms. b) Zoomed Far amplitude map for Pleistocene Prospect anomaly overlaid by depth structure contour map extracted at window (-10, 40) ms. c) Zoomed Near amplitude map for Pleistocene Prospect anomaly overlaid by depth structure contour map extracted at window (-10, 40) ms

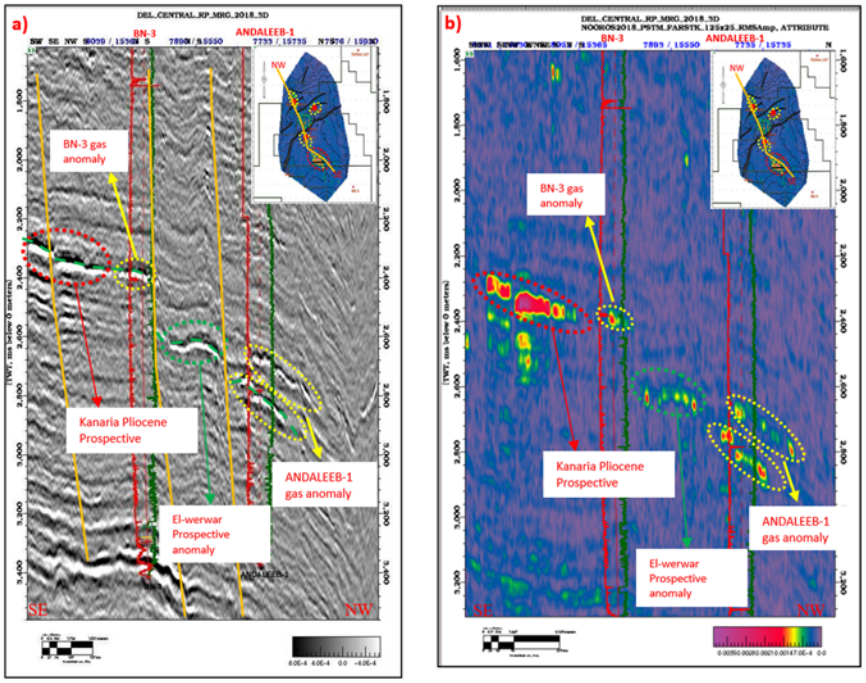

Fig. 18. a) SW-NE Seismic Section at full post-Stack Time Migration (PSTM), passing through Kanaria Pliocene Prospect, BN-3 and ANDALEEB-1wells b) SW-NE Seismic Section at Far-Post-Stack Time Migration (PSTM), passing through Kanaria Pliocene Prospect, BN-3 and ANDALEEB-1wells

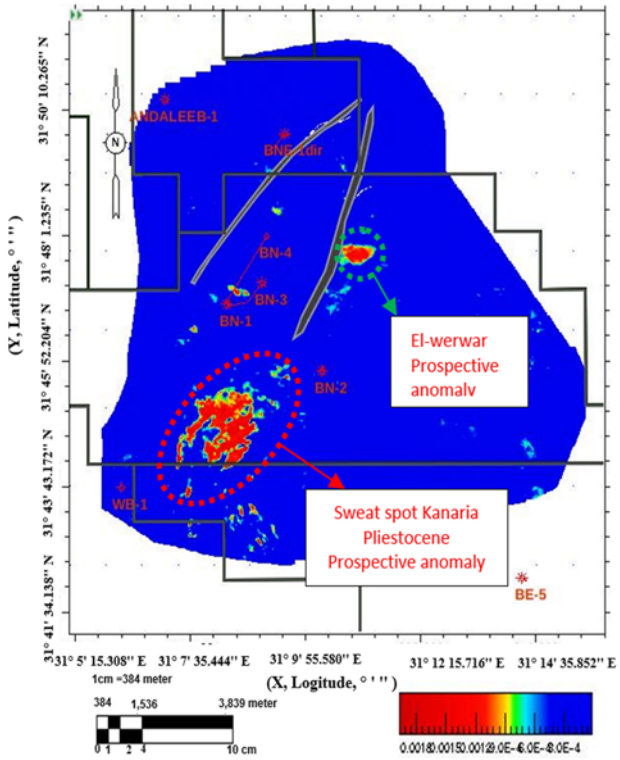

Fig. 19. Sweetness attribute map showing gas sand distribution at the Kanaria Pleistocene Anomaly, outlined in a red circle, with high sweetness values (in red) highlighting gas-bearing sands. The El Werwar prospective anomaly is outlined in green, indicating its potential for hydrocarbons

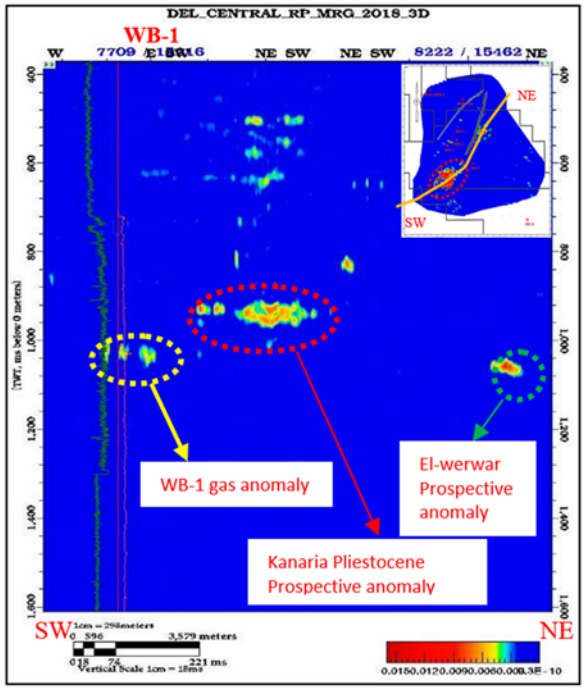

Fig. 20. SW-NE Sweetness attribute seismic section extracted at Far Post-Stack Time Migration (PSTM), passing through the Kanaria Pleistocene Prospect and WB-1 well. High sweetness values (orange to red) highlight the gas-bearing sands, confirming the presence of hydrocarbons at the Pleistocene anomaly.

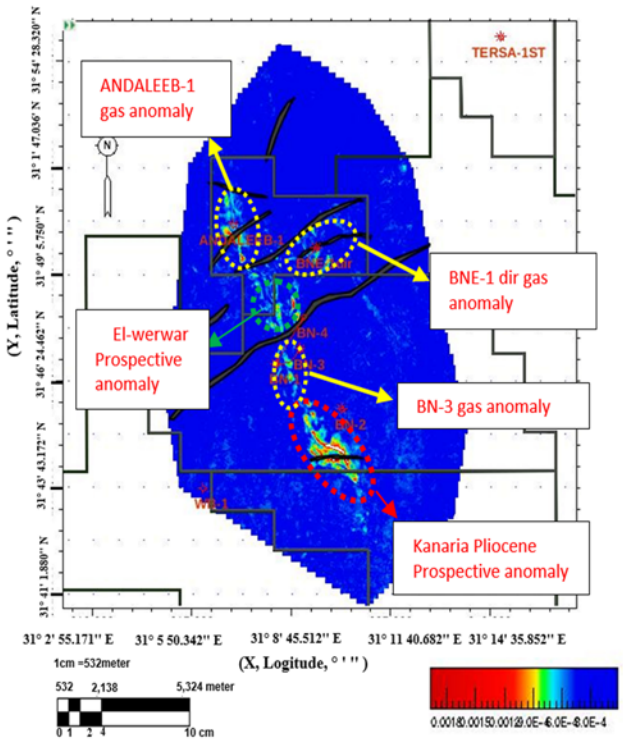

Fig. 21. Sweetness attribute map showing gas sand distribution at the Kanaria Pliocene Anomaly, outlined with a red circle, with high sweetness values (in red) highlighting the gas-bearing sands. The El Werwar prospective anomaly is outlined in green, indicating its hydrocarbon potential at this location

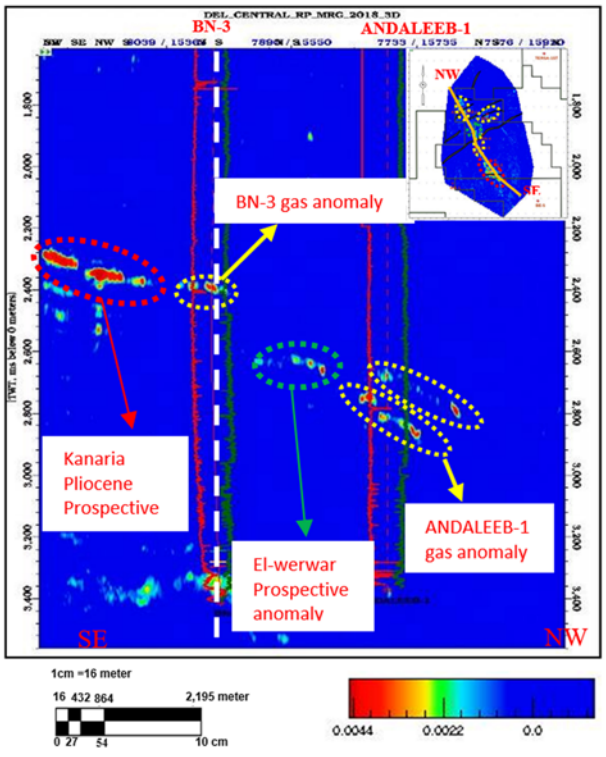

Fig. 22. SW-NE Sweetness attribute seismic section extracted at Far Post-Stack Time Migration (PSTM), passing through the Kanaria Pliocene Prospect, as well as the BN-3 and Andaleeb-1 wells. High sweetness values (orange to red) are observed, indicating the presence of hydrocarbons in the Pliocene anomaly.

amplitude, consistent with AVO Class III (Fig. 17a-c).

The arbitrary seismic section (SW-NE), created from far post-stack and RMS post-stack time migrations, highlights two discovery wells (BN-3 and ANDALEEB-1), indicated by a yellow circle, which aligns with the Kanaria and El-Werwar prospects (Fig. 18a-b). High-amplitude anomalies within the Pleistocene and Pliocene prospects, particularly at Kanaria and El-Werwar, provide a strong indication of gas reserves. To enhance confidence in these prospects, it is recommended that this amplitude map be supplemented with additional seismic properties.

The second type is the sweetness attribute is a key indicator of hydrocarbons, highlighting areas where seismic high frequencies are lost, which in turn outlines the channel morphology. This attribute helps interpret seismic horizons and identify hydrocarbon distribution.

For the Pleistocene anomaly, Fig. 19 shows the high sweetness values in the Kanaria Pleistocene prospect, outlined in red, indicating the gas-bearing sands. The El Werwar prospective anomaly is outlined in green in the same figure, highlighting its potential for hydrocarbons. Additionally, Fig. 20 shows a SW-NE seismic section passing through the Kanaria Pleistocene prospect and WB-1 well, confirming the hydrocarbon presence in this region. The section also indicates high sweetness values, further supporting the gas potential at the Kanaria anomaly.

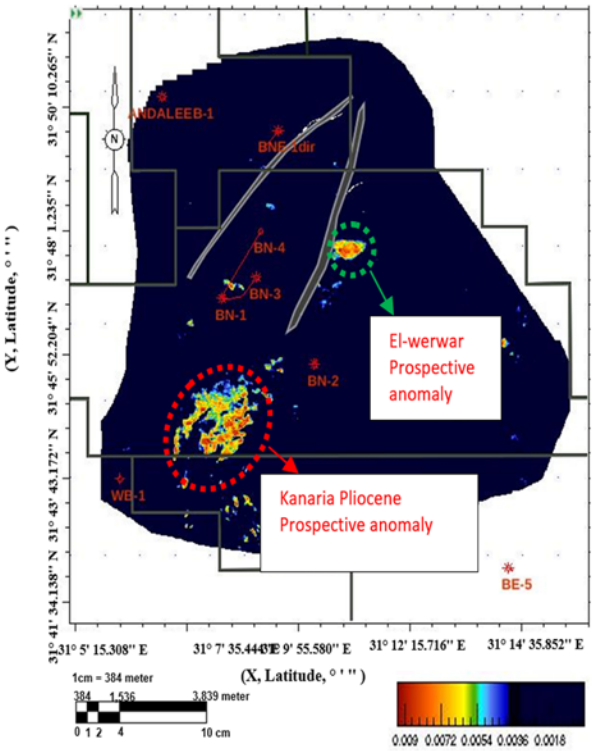

Fig. 23. Reflection Strength attribute map showing gas sand distribution for the Kanaria Pleistocene anomaly. The orange color, representing high reflectivity, corresponds to gas sands and is outlined with a red circle. The El Werwar prospective anomaly is outlined with a green circle, both anomalies appearing distinct against the darker background, which indicates lower reflectivity. The Kanaria anomaly is characterized by higher reflectivity, indicating gas presence in the Pleistocene formation

The second type is the sweetness attribute is a key indicator of hydrocarbons, highlighting areas where seismic high frequencies are lost, which in turn outlines the channel morphology. This attribute helps interpret seismic horizons and identify hydrocarbon distribution.

For the Pleistocene anomaly, Fig. 19 shows the high sweetness values in the Kanaria Pleistocene prospect, outlined in red, indicating the gas-bearing sands. The El Werwar prospective anomaly is outlined in green in the same figure, highlighting its potential for hydrocarbons. Additionally, Fig. 20 shows a SW-NE seismic section passing through the Kanaria Pleistocene prospect and WB-1 well, confirming the hydrocarbon presence in this region. The section

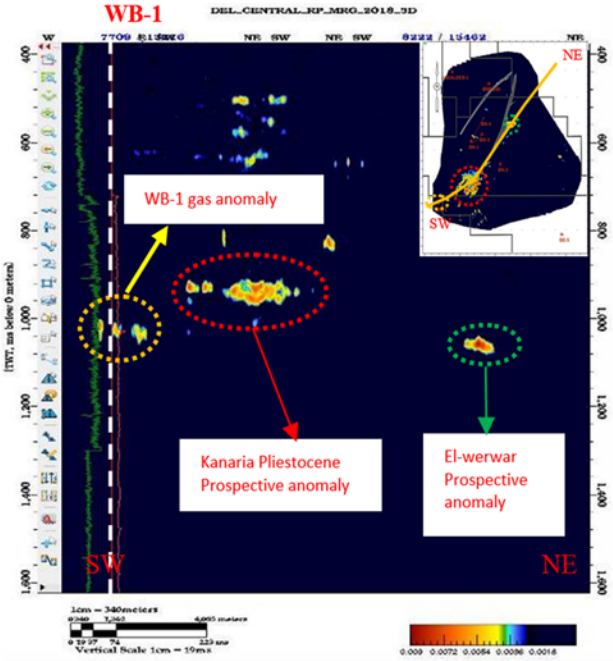

Fig. 24. SW-NE Reflection Strength Attribute Seismic Section (PSTM) passing d the El Werwar prospective anomaly. High reflectivity in these areas signifies gas-bearing sands.

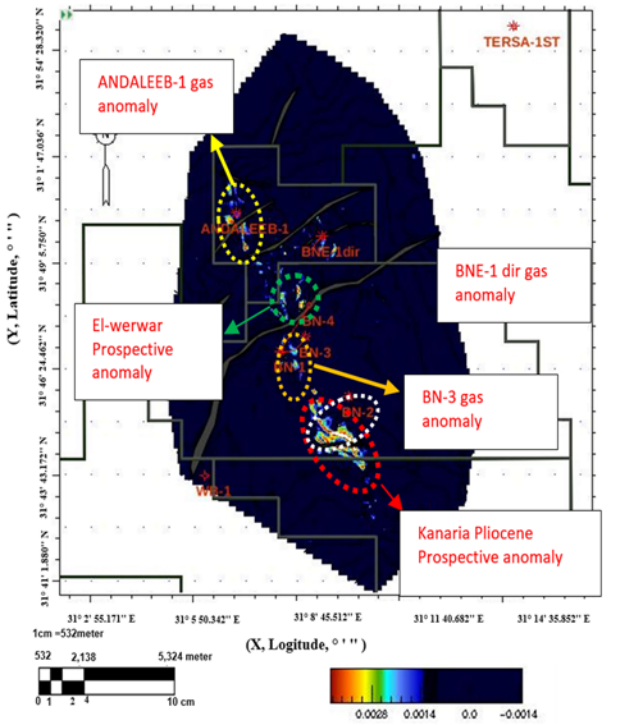

Fig. 25. Reflection Strength attribute map showing gas sand distribution at the Kanaria Pliocene prospect. The red circle outlines the Kanaria Pliocene anomaly, while the green circle marks the El Werwar prospective anomaly. Both anomalies exhibit high reflectivity (orange), indicating gas sands, and are clearly distinguishable from the surrounding darker reflectivity

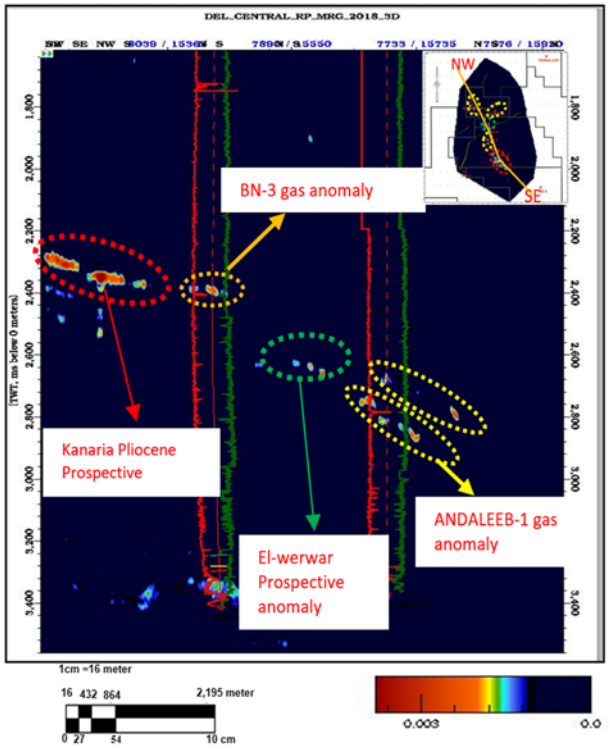

Fig. 26. SE-NW Reflection Strength Attribute Seismic Section (PSTM) passing through the Kanaria Pliocene prospect, El Werwar prospective anomaly, and proven gas anomalies at BN-3 and Andaleeb-1 wells. The high reflectivity (orange) marks the gas-bearing sands along these anomalies

also indicates high sweetness values, further supporting the gas potential at the Kanaria anomaly.

For the Pliocene anomaly, Fig. 21 shows the high sweetness values for the Kanaria Pliocene anomaly, outlined in red, while Fig. 22 displays the SW-NE seismic section passing through the Kanaria Pliocene prospect, along with the BN-3 and Andaleeb-1 wells, both of which are proven gas anomalies. This section further supports the hydrocarbon potential in the Kanaria Pliocene anomaly, as indicated by the high sweetness values and the presence of proven gas anomalies in the region.

The third type is the reflection strength attribute, where hydrocarbon-bearing areas are shown with a color range from yellow to orange, indicating low reflectivity. These areas correspond to gas sands with the lowest values on the reflection strength scale. As shown in Fig. 23, the first Pleistocene anomaly appears as high reflectivity in orange, which is outlined with a red circle to highlight the gas-bearing sands in the Kanaria prospect. In comparison, El Werwar, which is another prospective anomaly, is outlined by a green circle. These anomalies are easily distinguished from the background, which exhibits darker reflectivity, further emphasizing the presence of hydrocarbons.

Additionally, an arbitrary SW-NE seismic section, passing through the WB-1 well, reveals the presence of high reflectivity in orange, outlined with an orange circle to highlight the proven Pleistocene gas anomaly. This section demonstrates the relationship between the Kanaria Pleistocene anomaly, which also exhibits high reflectivity (outlined with a red circle), and the El Werwar prospective anomaly, outlined in green. The distinct contrast between these anomalies and the darker surrounding background further underscores the presence of hydrocarbons, emphasizing their potential for exploration.

In the Fig. 25, the Kanaria Pliocene anomaly is highlighted with high reflectivity in orange, marked by a red circle, while the El Werwar prospective anomaly is outlined in green. Both anomalies are clearly distinguishable from the

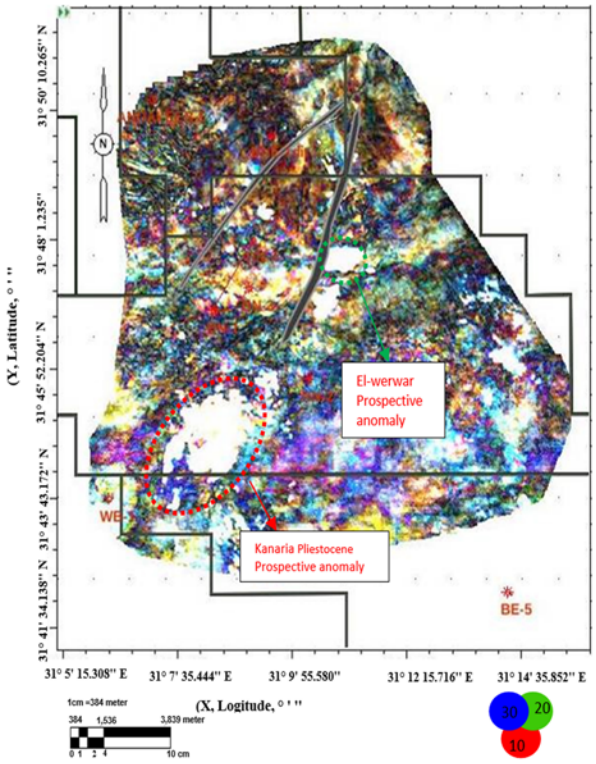

Fig. 27. Spectral Decomposition attribute map, RGB (10, 20, 30 Hz) frequencies show the channel gas sand distribution for the Kanaria Prospect, Pleistocene Anomaly. The white color represents the low-frequency Kanaria Pleistocene prospective anomaly, which is outlined by the red circle. The El-Werwar Pleistocene prospective anomaly is outlined by the green circle

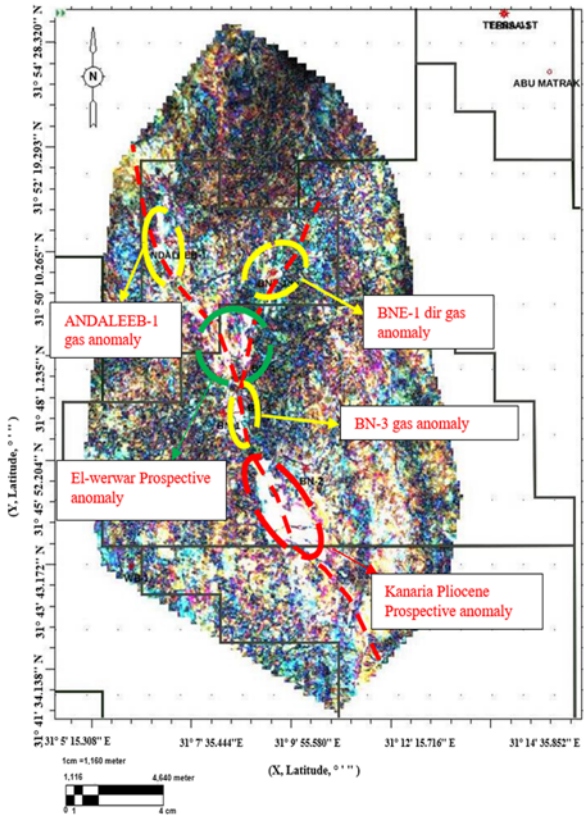

Fig. 28. Spectral Decomposition attribute map, RGB (20, 30, 40) Hz frequencies, showing the Pliocene channelized fairway distribution. The red dashed lines represent the distributary fairway channel of the Pliocene Kanaria prospect, with the main fairway trending from SW to NE, passing through the Kanaria Pliocene prospect, the El Werwar prospective anomaly, and the BN-3 and Andaleeb-1 gas anomalies, which are proven gas accumulations along the main Pliocene channel. Additionally, a northeastern branch of the main fairway is indicated by dashed lines, which passes through the BNE-1 dir proven gas anomaly, located along the branched channel

darker surrounding reflectivity, suggesting the presence of gas sands.

Additionally, Fig. 26 presents an arbitrary SE-NW seismic section, passing through both the Kanaria Pliocene anomaly and El Werwar prospective anomaly, as well as two proven gas anomalies at the BN-3 and Andaleeb-1 wells. This section clearly shows high reflectivity in these areas, confirming the gas-bearing nature of the anomalies and supporting their potential for hydrocarbon exploration.

The fourth type is the spectral decomposition attribute, applied using RGB color-bending maps for both Pleistocene and Pliocene anomalies, which creates an image composed of three detected frequency horizons that identify the channel fairway direction. The first Pleistocene anomaly is composed of 10, 20, and 30 Hz frequencies, shown in Fig. 27, which highlights the turbidity gas sand feature for the Pleistocene Kanaria prospect. In this map, the white color represents the low-frequency Kanaria Pleistocene prospective anomaly, outlined by the red circle. Additionally, the El-Werwar Pleistocene prospective anomaly is marked by a green circle, and the second Pliocene anomaly is composed of 20, 30, and 40 Hz frequencies, shown in Fig. 28, which illustrates the channelized fairway flow of the Pliocene anomaly. The main fairway follows a southwest-to-northeast trend, passing through key locations such as the Kanaria Pliocene prospect, the El Werwar prospective anomaly, and the BN-3 and Andaleeb-1 gas anomalies, which are proven gas accumulations along the main Pliocene channel. In addition, a northeastern branch of the main fairway, indicated in the spectral decomposition map, passes through the BNE-1 dir proven gas anomaly, situated along the branched channel.

Table 1. Summary of Key Findings for Structural and Stratigraphic Seismic Attributes in the Baltim Area: Pleistocene and Pliocene Anomalies

Seismic Attribute	Category	Key Findings	Application/Insight
Discontinuity	Structural	Identified fault systems and discontinuities in the subsurface.	Useful for detecting fault zones, especially in the El Wastani and Kafr El-Sheikh formations.
Fault Likelihood (FLH)		Revealed fault sealing properties, distinguishing between sealed, partially sealed, and non-sealed fault	Essential for assessing gas migration potential and fault behavior.
Sweetness	Stratigraphic	Highlighted zones of high frequencies loss, indicative of gas-bearing sands.	Critical for identifying gas zones and channelized sands in the Pleistocene and Pliocene anomalies.
Reflection Strength		Enhanced visibility of gas-bearing zones with high reflectivity.	Key for differentiating between gas-bearing sands and other geological layers.
Spectral Decomposition		Clarified the Pliocene channel fairway, gas-bearing sands, and turbidity associated with anomalies.	Important for delineating channelized reservoirs and assessing hydrocarbon potential.

Table 1 presents a comprehensive summary of the key findings related to the structural and stratigraphic seismic attributes in the Baltim area. It includes a detailed overview of the Pleistocene and Pliocene anomalies, with all the structural and stratigraphic attributes used in the study summarized for clarity and reference.

COMPARISON WITH PREVIOUS STUDIES

This study applies a novel combination of structural and stratigraphic seismic attributes to delineate gas-bearing reservoirs in the Plio-Pleistocene succession of the Baltim Gas Field, Nile Delta. We integrate discontinuity, fault likelihood, sweetness, reflection strength, and spectral decomposition to enhance gas reservoir identification. Below is a comparison of our methodology with similar research in the Nile Delta.

Structural Seismic Attributes: Discontinuity

The application of discontinuity attributes for fault detection is well-documented in studies by Imran et al. (2021). While their study focused on fault detection, our research further integrates fault likelihood (FLH) to assess fault sealing, allowing us to categorize faults as fully sealed, partially sealed, or non-sealed. This provides a more refined approach to understanding fault behavior and its influence on gas accumulation, particularly in the Plio-Pleistocene gas reservoirs.

Stratigraphic Seismic Attributes: Spectral Decomposition and Sweetness

Previous studies, such as Noureldin et al. (2023) have used spectral decomposition to identify geological features like channelized reservoirs. While spectral decomposition was also used in our study, we combined it with sweetness and reflection strength to more effectively identify gas-bearing sands and differentiate hydrocarbon zones. This integrated approach improves reservoir delineation and provides a more robust method for exploring gas anomalies.

Seismic Attributes in the Nile Delta

The use of seismic attributes in the Nile Delta, as explored by Sarhan and Safa (2017), primarily focused on fault and stratigraphic analysis in the Kafr El Sheikh formation. Unlike these studies, our research integrates a wider array of seismic attributes, providing a comprehensive understanding of both structural and stratigraphic components of gas reservoirs. This holistic approach enables a more accurate assessment of gas accumulation in the Pleistocene and Pliocene anomalies.

Summary of Comparison

In summary, this study expands on previous work by integrating a broader suite of seismic attributes, offering a more comprehensive and nuanced approach to gas reservoir delineation. The combination of discontinuity, fault likelihood, sweetness, reflection strength, and spectral decomposition provides a more precise

and detailed methodology for identifying gas-bearing zones in the Plio-Pleistocene succession of the Baltim Gas Field.

DISCUSSION AND CONCLUSION

This study focuses on identifying prospective anomalies in the shallow reservoir of the Baltim field using a combination of structural and stratigraphic seismic attributes. Spectral decomposition, based on seismic frequencies, clarifies the Pliocene channel fairway, gas-bearing sands, and the turbidity associated with the first Pleistocene anomaly. However, a critical evaluation of the limitations in the seismic data, especially in regions near the shoreline, is necessary. In areas with a lower signal-to-noise ratio, interpretation accuracy may be compromised, particularly for small or subtle anomalies. Furthermore, the complexity of the geological setting, including fault systems and lithological variations, introduces uncertainty regarding the continuity and extent of gas reservoirs. The impact of these data limitations and geological complexities should be carefully considered to assess how they could influence the study's conclusions about gas accumulation in the Baltim field.

The first El Wastani prospect measures approximately 5,209 m², while the second Pliocene prospect spans 5,488 m², with a fault line separating them. These findings provide a significant foundation for future hydrocarbon exploration in the region. Based on these results, similar methodologies could be applied to explore other deltaic or offshore areas, potentially broadening the understanding of gas-bearing reservoirs and fault sealing mechanisms.

In addition to its application in the Baltim field, the methodologies and findings of this study have broader implications for gas exploration in similar geological settings. The combination of structural and stratigraphic seismic attributes, including spectral decomposition and amplitude mapping, can be applied to other deltaic and offshore regions with comparable tectonic and sedimentary environments. This approach may improve gas exploration in Mediterranean basins or other tectonically active areas where fault systems and sedimentary structures are critical for reservoir formation. Furthermore, the techniques used to identify fault sealing mechanisms and gas-bearing sands could improve the precision of reservoir delineation in complex offshore environments globally. Based on these findings, extending these methods to similar geological contexts could enhance hydrocarbon exploration, especially in regions with high exploration potential but challenging subsurface conditions.

LIMITATIONS AND FUTURE DIRECTIONS

This study provides valuable insights into the hydrocarbon potential of the Baltim field, but some limitations need to be addressed:

1. *Seismic Resolution:* The seismic data, particularly near the shoreline, has a lower signal-to-noise ratio, which reduces the accuracy of attribute interpretation and makes it harder to identify small anomalies.
2. *Seismic Attribute Limitations:* While attributes like RMS Amplitude are useful for detecting gas accumulations, they may not fully capture the complexity of reservoirs with varying lithology and structure. Additionally, very thin reservoirs may be difficult to detect due to the limitations of seismic resolution.
3. *Geological Complexity:* The Baltim field's complex geology, including fault systems and lithological variations, means that seismic data alone may not provide a complete reservoir characterization. Additional geological data are needed for more accurate interpretations.

Future Research Directions

1. *Improved Seismic Data:* Future studies should aim to collect higher-quality seismic data, especially in areas with low signal-to-noise ratios, to improve resolution.
2. *Advanced Seismic Techniques:* Using more advanced seismic methods, such as Full Waveform Inversion (FWI), could enhance resolution and help identify reservoir features more accurately.
3. *Integration with Geological Data:* Combining seismic data with geological and geochemical information (such as

core analysis) would improve seismic interpretation and provide a more accurate subsurface understanding.

By addressing these limitations and pursuing these directions, seismic attributes can be better applied in hydrocarbon exploration, leading to more accurate identification of potential reservoirs in the Baltim field.

ACKNOWLEDGEMENT

The Researchers desire to convey their appreciation to the Belayim Petroleum Company, the Egyptian General Petroleum Corporation (EGPC), and the Geophysics Department of Cairo University for their aid in the dissemination of this research.

Competing interests: No financial and non-financial competing interests.

Data availability: Data can be requested from Mr. Aly Saeed ali El-sayed, the first author of the article

REFERENCES

Aal, A.A., El Barkooky, A., Gerrits, M., Meyer, H., Schwander, M., Zaki, H. 2000. Tectonic evolution of the Eastern Mediterranean Basin and its significance for hydrocarbon prospectivity in the ultradeepwater of the Nile Delta. The leading Edge, vol. 19(10), p. 1086-1102. https://doi.org/10.1190/1.1438485

Abd El-Gawad, E.A., Abdelwahhab, M.A., Bekiet, M.H., Noah, A.Z., ElSayed, N.A., Fouda, A.E.E. 2019. Static reservoir modeling of El Wastani formation, for justifying development plans, using 2D seismic and well log data in Scarab field, offshore Nile Delta, Egypt. Journal of African Earth Sciences, vol. 158, 103546. https://doi.org/10.1016/j.jafrearsci.2019.103546

Abdel-Fattah, M.I., Hamdan, H.A., Sarhan, M.A. 2023. Hydrocarbon potential and reservoir characteristics of incised-valley transgressive sandstones: A case study of the Messinian gas reservoirs (Nile Delta Basin, Egypt). Journal of African Earth Sciences, vol. 207, 105073. https://doi.org/10.1016/j.jafrearsci.2023.105073

Abdel-Fattah, M.I., Tawfik, A.Y. 2015. 3D geometric modeling of the Abu Madi reservoirs and its implication on the gas development in Baltim Area (Offshore Nile Delta, Egypt). International Journal of Geophysics, vol. 2015(1), 369143. https://doi.org/10.1155/2015/369143

Abdulkareem, L.N. 2022. AVO analysis for high amplitude anomalies using 2D pre-stack seismic data. Kuwait Journal of Science, vol. 49(2),12351. https://doi.org/10.48129/kjs.12351

Akinwale, R.P., Ayolabi, E., Akinwale, S.A. 2022. 3D structural modelling and spectral decomposition analysis of Jay Field offshore Niger Delta, Nigeria. Journal of Engineering and Applied Science, vol. 69(1), 91. https://doi.org/10.1186/s44147-022-00147-8

Almasgari, A.A., Elsaadany, M., Latiff, A.H.A., Hermana, M., Rahman, A.H.B.A., Babikir, I., Imran, Q.S., Appiah, N.F., Adeleke, T.O. 2020. Application of seismic attributes to delineate the geological features of the Malay Basin. Bulletin of the Geological Society of Malaysia, vol. 69, p. 97-110. https://doi.org/10.7186/bgsm69202009

Alotaibi, N., Metwally, A. 2024. Delineation of Subsurface Structures using Seismic Refraction Tomographic Inversion in Wadi Al-Dawasir, South Saudi Arabia. Engineering Technology and Applied Science Research, vol. 14(5), p. 16519-16526. https://doi.org/10.48084/etasr.7915

Amer, M., Mabrouk, W.M., Soliman, K.S., Noureldin, A.M., Metwally, A. 2023. Three-Dimensional Integrated Geo-Static Modeling for Prospect Identification and Reserve Estimation in the Middle Miocene Multi-Reservoirs: A Case Study from Amal Field, Southern Gulf of Suez Province. Natural Resources Research, vol. 32. p. 2609-2635. https://doi.org/10.1007/s11053-023-10253-w

Amer, M., Mabrouk, W.M., Soliman, K.S., Eid, A.M., Metwally, A. 2024. Formation evaluation of middle Miocene reservoirs via petrophysical analysis of well logging data; case study from Southern part of Gulf of Suez, Egypt. 18. 39-57. https://doi.org/10.30499/IJG.2023.409210.1532

Azeem, T., Yanchun, W., Khalid, P., Xueqing, L., Yuan, F., Lifang, C. 2015. An application of seismic attributes analysis for mapping of

gas bearing sand zones in the sawan gas field, Pakistan. Acta Geodaetica Et Geophysica, vol. 51(4), 723-744. https://doi.org/10.1007/s40328-015-0155-z

Barakat, M. 2010. Modern geophysical techniques for constructing a 3D geological model on the Nile Delta, Egypt. PhD thesis, Technical University, Berlin, Germany, 144 p.

Barakat, M., Dominik, W. 2010. Seismic Studies on the Messinian Rocks in the Onshore Nile Delta, Egypt. 72nd EAGE Conference and Exhibition Incorporating SPE EUROPEC 2010. https://doi.org/10.3997/2214-4609.201401362

Barakat, M.K., El-Gendy, N.H., El-Bastawesy, M.A. 2019. Structural modeling of the Alam EL-Bueib Formation in the jade oil field, Western Desert, Egypt. Journal of African Earth Sciences, vol. 156, p. 168-177. https://doi.org/10.1016/j.jafrearsci.2019.05.003

Castagna, J.P., Sun, S., Siegfried, R.W. 2003. Instantaneous spectral analysis: Detection of low-frequency shadows associated with hydrocarbons. The Leading Edge, vol. 22(2), p. 120-127. https://doi.org/10.1190/1.1559038

Chen, Q., Sidney, S. 1997. Seismic attribute technology for reservoir forecasting and monitoring, The Leading Edge, vol. 16(5), p. 445-456. https://doi.org/10.1190/1.1437657

Chopra, S., Marfurt, K.J. 2005b. Seismic attributes - A historical perspective. Geophysics, vol. 70(5), p. 3SO-28SO. https://doi.org/10.1190/1.2098670

Chopra, S., Marfurt, K.J. 2007. Seismic Attributes for Prospect Identification and Reservoir Characterization. Society of Exploration Geophysicists, Geophysical Developments Series, p 481. https://doi.org/10.1190/1.9781560801900

Coren, F., Volpi, V., Tinivella, U. 2001. Gas hydrate physical properties imaging by multi-attribute analysis - Blake Ridge BSR case history. Marine Geology, vol. 178(1-4), p. 197-210. https://doi.org/10.1016/S0025-3227(01)00156-6

Del Moro, Y. 2012. An integrated seismic, geologic and petrophysical approach to characterize the Red Fork incise valley fill system in the Anadarko Basin, Oklahoma. Unpublished M.Sc thesis, University of Oklahoma, USA, 121 p.

Eid, A.M., Mabrouk, W.M., Amer, M., Metwally, A. 2023. 3D structural modeling using seismic data and well logs for Khatatba reservoir in Matruh-Shushan Basin, North Western Desert, Egypt. Scientific Reports, vol. 13, 20158. https://doi.org/10.1038/s41598-023-47487-w

Eid, A.M., Mabrouk, W. M., Metwally, A. 2024. Formation Evaluation and Petrophysical Analysis of Well Logging Data: An Example from Matruh-Shushan Basin, North Western Desert, Egypt. Iraqi Journal of Science, vol. 65(8), p. 4336-4358. https://doi.org/10.24996/ijs.2024.65.8.18 https://doi.org/10.24996/ijs.2024.65.8.18

El-Ata, A.S.A., El-Gendy, N.H., El-Nikhely, A.H., Raslan, S.M., El-Oribi, M.S., Barakat, M.K. 2023. Seismic characteristics and AVO response for non-uniform Miocene reservoirs in offshore eastern Mediterranean region, Egypt. Scientific Reports, vol. 13(1). 8897. https://doi.org/10.1038/s41598-023-35718-z

El-Ella R.A. 1990. The Neogene-quaternary section in the Nile delta, Egypt: geology and hydrocarbon potential. Journal of Petroleum Geology, vol. 13(3), p. 329-340. https://doi.org/10.1306/BF9AB6CE-0EB6-11D7-8643000102C1865D

El-Fawal, F.M., Sarhan, M.A., Collier, R.E.L., Basal, A., Aal, M.H.A. 2016. Sequence stratigraphic evolution of the post-rift MEGASEQUENCE in the northern part of The Nile Delta basin, Egypt. Arabian Journal of Geosciences, vol. 9, p. 585. https://doi.org/10.1007/s12517-016-2602-8

El-Gendy, N., El-Nikhely, A., Zakaria, A., Hellish, H., Nabawy, B., Barakat, M. 2023. Pre-Stack Imaging for the Messinian Sub Salt Sequences in the Levantine Basin of the East Mediterranean: A Case Study, Offshore Lebanon. Iraqi Geological Journal, vol. 56(1F), p. 1-18. https://doi.org/10.46717/igj.56.1F.1ms-2023-6-9

El-Hameedy, M.A., Mabrouk, W.M., Dahroug, S., Youssef, M.S., Metwally, A.M. 2023. Role of Seismic Refraction Tomography (SRT) in bedrock mapping; case study from industrial zone, Ain-Sokhna area, Egypt.

Contributions to Geophysics and Geodesy, vol. 53(2), p. 11-128. https://doi.org/10.31577/congeo.2023.53.2.2

El-Nikhely, A., El-Gendy, N.H., Bakr, A.M., Zawra, M.S., Ondrak, R., Barakat, M.K. 2022. Decoding of seismic data for complex stratigraphic traps revealing by seismic attributes analogy in Yidma/Alamein concession area Western Desert, Egypt. Journal of Petroleum Exploration and Production Technology, vol. 12(12), p. 3325-3338. https://doi.org/10.1007/s13202-022-01527-9

El-Saoud, A.A., Helal, A.E.N., Matresu, J., Lala, A.M.S. 2022. Applications of Amplitude versus Offset and Seismic Attributes for Perceiving Messinian Reservoirs in Nidoco Field, Nile Delta, Egypt. International Journal of Geosciences, vol. 13(05), p. 319-328. https://doi.org/10.4236/ijg.2022.135017

El-Sayed Ali, S., Mabrouk, W.M., Metwally, A.M. 2024. Utilizing post-stack seismic inversion for delineation of gas-bearing sand in a pleistocene reservoir, baltim gas field, nile delta, Egypt. Scientific Reports, vol. 14, 29596. https://doi.org/10.1038/s41598-024-78186-9

Emujakporue, G.O., Enyenihi, E.E. 2020. Identification of seismic attributes for hydrocarbon prospecting of Akos field, Niger Delta, Nigeria. SN Applied Sciences, vol. 2(5), p. 910. https://doi.org/10.1007/s42452-020-2570-1

Ewing, T.E. 2001. Synthetic seismograms: Preparation, Calibration, and Associated issues. AAPG Explorer, p. 2017-2043.

Farfour, M., El-Ghali, M.A.K., Gaci, S., Moustafa, M.S.H., Siddiqui, N.A. 2021. Seismic attributes for hydrocarbon detection and reservoir characterization: a case study from Poseidon field, Northwestern Australia. Arabian Journal of Geosciences, vol. 14, p. 2814. https://doi.org/10.1007/s12517-021-08853-y

Ghosh, D., Halim, M.F.A., Brewer, M., Viratno, B., Darman, N. 2010. Geophysical issues and challenges in Malay and adjacent basins from an E & P perspective. The Leading Edge, vol. 29(4), p. 436-449. https://doi.org/10.1190/1.3378307

Hale, D. 2013. Methods to compute fault images, extract fault surfaces, and estimate fault throws from 3D seismic images. Geophysics, vol. 78(2), O33-O43. https://doi.org/10.1190/geo2012-0331.1

Harris, R., Bracken, K., Miller, B., Angelovich, S., O'Toole, T. 2019. Subseismic Fault Identification Using the Fault Likelihood Attribute: Application to Geosteering in the DJ Basin. Proceedings of the 7th Unconventional Resources Technology Conference Denver, Colorado, 22-24 July 2019. https://doi.org/10.15530/urtec-2019-602

Hart, B.S. 2008. Channel detection in 3-D seismic data using sweetness. AAPG Bulletin, vol, 92(6), 733-742. https://doi.org/10.1306/02050807127

Hesham, A., Fattah, N.A., Dahroug, A. 2023. Integrating seismic attributes and rock physics for delineating Pliocene reservoir in Disouq field, Nile Delta, Egypt. Contributions to Geophysics and Geodesy, vol. 53(1), p. 65-84. https://doi.org/10.31577/congeo.2023.53.1.4

Hossain, S. 2019. Application of seismic attribute analysis in fluvial seismic geomorphology. Journal of Petroleum Exploration and Production Technology, vol. 10(3), p. 1009-1019. https://doi.org/10.1007/s13202-019-00809-z

Ibekwe, K.N., Arukwe, M.C., Ahaneku, C.V., Onuigbo, E., Omoareghan, J.O., Lanisa, A., Oguadinma, V.O. 2023. The application of seismic attributes in fault detection and direct hydrocarbon indicator in Tomboy Field, Western Offshore Niger Delta Basin. Journal of Energy Research and Reviews, vol. 14(2), p. 9-23. https://doi.org/10.9734/jenrr/2023/v14i2279

Imran, Q.S., Siddiqui, N.A., Latiff, A.H.A., Bashir, Y., Khan, M., Qureshi, K., Al-Masgari, A.A.S., Ahmed, N., Jamil, M. 2021. Automated Fault Detection and Extraction under Gas Chimneys Using Hybrid Discontinuity Attributes. Applied Sciences, vol. 11(16), 7218. https://doi.org/10.3390/app11167218

Ismail, A., Ewida, H.F., Al-Ibiary, M.G., Zollo, A. 2020. Integrated prediction of deep-water gas channels using seismic coloured inversion and spectral decomposition attribute, West

offshore, Nile Delta, Egypt. NRIAG Journal of Astronomy and Geophysics, vol. 9(1), p. 459-470. https://doi.org/10.1080/20909977.2020.1768324

Kadi, H.H.E., Shebl, S., Ghorab, M., Azab, A., Salama, M. 2020. Evaluation of Abu Madi Formation in Baltim North & East gas fields, Egypt, using seismic interpretation and well log analysis. NRIAG Journal of Astronomy and Geophysics, vol. 9(1), p. 449-458. https://doi.org/10.1080/20909977.2020.1765275

Kamel, H., Eita T., Sarhan, M. 1998. Nile Delta hydrocarbon potentiality. In: Proc. EGPC, 14th Petroleum Exploration and Production Conference, vol. 2, p. 485-503.

Kington, J. 2015. Semblance, coherence, and other discontinuity attributes. The Leading Edge, vol. 34(12), p. 1426-1544. https://doi.org/10.1190/tle34121510.1

Kirschbaum, M.A., Schenk, C.J., Charpentier, R.R., Klett, T.R., Brownfield, M.E., Pitman, J.K., Cook, T.A., Tennyson, M.E. 2010. Assessment of undiscovered oil and gas resources of the Nile Delta Basin Province, Eastern Mediterranean. Fact Sheet 2010-3027, World Petroleum Resources Project. U.S. Geological Survey. https://doi.org/10.3133/fs20103027

Koson, S., Chenrai, P., Choowong, M. 2021. Seismic Attributes and Their Applications in Seismic Geomorphology. Bulletin of Earth Sciences of Thailand, vol. 6(1), p. 1-9. https://ph01.tci-thaijo.org/index.php/bestjournal/issue/view/16858

Lasheen, I., Noureldin, A.M., Metwally, A. 2024. Reservoir characterization of the Abu Roash D Member through petrography and seismic interpretations in Southern Abu Gharadig Basin, Northern Western Desert, Egypt. Scientific Reports, vol. 14(1), p. 8966. https://doi.org/10.1038/s41598-024-58846-6

Laughlin, K., Garossino, P., Partyka, G. 2002. Spectral decomposition applied to 3D. AAPG Explorer, vol. 23(5), p. 28-31.

Lasheen, I.; Noureldin, A. M.; Metwally, A.; 2024. Reservoir characterization of the Abu Roash D Member through petrography and seismic interpretations in Southern Abu Gharadig Basin, Northern Western Desert, Egypt. Scientific Reports, 14(1), 8966. https://doi.org/10.1038/s41598-024-78186-9

Lasheen, I.; Noureldin, A. M.; Metwally, A.; 2024. Reservoir characterization of the Abu Roash D Member through petrography and seismic interpretations in Southern Abu Gharadig Basin, Northern Western Desert, Egypt. Scientific Reports, 14(1), 8966. https://doi.org/10.1038/s41598-024-78186-9

Lou, Y., Zhang, B., Wang, R., Lin, T., Cao, D. 2019. Seismic fault attribute estimation using a local fault model. Geophysics, vol. 84(4), p. 1JA-Z21. https://doi.org/10.1190/geo2018-0678.1

Mahmoud, A.I., Metwally, A.M., Mabrouk, W.M., Leila, M. 2023. Controls on hydrocarbon accumulation in the pre-rift Paleozoic and late syn-rift Cretaceous sandstones in PTAH oil field, North Western Desert, Egypt: Insights from seismic stratigraphy, petrophysical rock-typing, and organic geochemistry. Marine and Petroleum Geology, vol. 155, 106398. https://doi.org/10.1016/j.marpetgeo.2023.106398

Makled, W.A., Mandur, M.M., Langer, M.R. 2017. Neogene sequence stratigraphic architecture of the Nile Delta, Egypt: A micropaleontological perspective. Marine and Petroleum Geology, vol. 85, p. 117-135. https://doi.org/10.1016/j.marpetgeo.2017.04.017

McArdle, N., Ackers, M. 2012. Understanding seismic thin-bed responses using frequency decomposition and RGB blending. First Break, vol. 30(12). https://doi.org/10.3997/1365-2397.2012022

Mohamed, H., Mabrouk, W.M., Metwally, A. 2024. Delineation of the reservoir petrophysical parameters from well logs validated by the core samples case study Sitra field, Western Desert, Egypt. Scientific Reports, vol. 14(1), 26841. https://doi.org/10.1038/s41598-024-77371-0 https://doi.org/10.1038/s41598-024-77371-0

Naseer, T.M., Radwan, A.E., Naseem, Sh. 2022. Seismic attributes and static reservoir simulation applications for imaging the thin-bedded stratigraphic systems of the Lower-Cretaceous Lower GORU fluvial resources, Pakistan. Journal of Asian Earth Sciences, vol. 240, 105409. https://doi.org/10.1016/j.jseaes.2022.105409

Nissen, S.E. 2002. Seismic Attributes for the Explorationist. Kansas Geological Survey: Open-file Report No. 2002-49.

Noureldin, A.M., Mabrouk, W.M., Metwally, A. 2023. Delineating tidal channel feature using integrated post-stack seismic inversion and spectral decomposition applications of the upper cretaceous reservoir Abu Roash C: A case study from Abu-Sennan oil field, Western Desert, Egypt. Journal of African Earth Sciences, vol. 205, 104974. https://doi.org/10.1016/j.jafrearsci.2023.104974

Okocha, F.O., Atakpo E. 2017. Effect of hydrocarbon production on reflection amplitude propertis of reservoirs-a case of Kov Field, Niger Delta, Nigeria. Arabian Journal of Geosciences, vol. 10, 380. https://doi.org/10.1007/s12517-017-3171-1

Oliveros, R.B., Radovich, B.J. 1997. Image-processing display techniques applied to seismic instantaneous attributes over the Gorgon gas field, North West Shelf, Australia. SEG Technical Program Expanded Abstracts 1997. https://doi.org/10.1190/1.1885862

Oumarou, S., Mabrouk, D., Tabod, T.C., Marcel, J., Ngos, S.III., Essi, J.M.A., Kamguia, J. 2021. Seismic attributes in reservoir characterization: an overview. Arabian Journal of Geosciences, vol. 14, p. 402. https://doi.org/10.1007/s12517-021-06626-1

Peyton, L., Bottjer, R. Partyka, G. 1998. Interpretation of incised valleys using new 3-D seismic techniques: A case history using spectral decomposition and coherency. The Leading Edge, vol 17(9), p. 1294-1298. https://doi.org/10.1190/1.1438127

Pwavodi, J., Kelechi, I.N., Angalabiri, P., Emeremgini, S.C., Oguadinma, V.O. 2023. Pore pressure prediction in offshore Niger delta using data-driven approach: Implications on drilling and reservoir quality. Energy Geoscience, vol. 4(3), 100194. https://doi.org/10.1016/j.engeos.2023.100194

Rizzini, A., Vezzani, F., Cococcetta, V., Milad, G. 1978. Stratigraphy and sedimentation of a Neogene-Quaternary section in the Nile Delta area (A.R.E.). Marine Geology, vol. 27(3-4), p. 327-348. https://doi.org/10.1016/0025-3227(78)90038-5

Roshdy, E., Mabrouk, W., Metwally, A. 2022. Application of Noise Attenuation on 2D Shallow Offshore Seismic Reflection Data: A Case Study from the Baltic Sea. Engineering, Technology and Applied Science Research, vol. 12(2), p. 8431-8434. https://doi.org/10.48084/etasr.4748

Sarhan, M.A. 2017. The efficiency of seismic attributes to differentiate between massive and non-massive carbonate successions for hydrocarbon exploration activity. NRIAG Journal of Astronomy and Geophysics, 6(2), p. 311-325. https://doi.org/10.1016/j.nrjag.2017.06.003

Sarhan, M.A. 2021a. Assessing hydrocarbon prospects in Abu Madi formation using well logging data in El-Qara field, Nile Delta Basin, Egypt. Journal of Petroleum Exploration and Production Technology, 11(6), p. 2539-2559. https://doi.org/10.1007/s13202-021-01214-1

Sarhan, M.A. 2021b. Gas-generative potential for the post-Messinian megasequence of Nile Delta Basin: a case study of Tao Field, North Sinai Concession, Egypt. Journal of Petroleum Exploration and Production Technology, vol. 12(4), p. 925-947. https://doi.org/10.1007/s13202-021-01354-4

Sarhan, M.A. 2022. New prospective gas plays in Pliocene sands, offshore Nile Delta Basin: A case study from Kamose-1 well at North Sinai Concession, Egypt. Petroleum Research, vol. 7(3), p. 329-340. https://doi.org/10.1016/j.ptlrs.2021.12.007

Sarhan, M.A., Safa, M.G. 2017. Application of Seismic Attributes for Detecting Different Geologic Features within Kafr El Sheikh Formation, Temsah Concession, Nile Delta Basin. Scientific Journal for Damietta Faculty of Science, vol. 7(1), p. 26-34. https://doi.org/10.21608/sjdfs.2017.194770

Sestini, G. 1989. Nile Delta: a review of depositional environments and geological history. Geological Society, London, Special Publications, vol. 41(1), p. 99-127. https://doi.org/10.1144/GSL.SP.1989.041.01.09

Sheriff, R.E. 1994. Encyclopedic dictionary of exploration geophysics. Society of Exploration Geophysicists, 89-94.

Subrahmanyam, D., Rao, P.H. 2008. Seismic Attributes - A Review. International

Conference and Exposition on Petroleum Geophysics, 398-405. https://spgindia.org/2008/398.pdf

Veeken, P.C.H. 2007. Seismic stratigraphy, basin analysis and reservoir characterization. In Helbig, K, Treitel S. (eds.), Handbook for Geophysical Exploration, Seismic Exploration, vol. 37, 507 p, Elsevier.

Zelenika, K.N., Mavar, K.N., Brnada, S. 2018. Comparison of the sweetness seismic attribute and porosity-thickness maps, Sava depression, Croatia. Geosciences, vol. 8(11), 426. https://doi.org/10.3390/geosciences8110426